Cleaner Materials 9 (2023) 100193

Contents lists available at ScienceDirect

Cleaner Materials

journal homepage: www.journals.elsevier.com/cleaner-materials

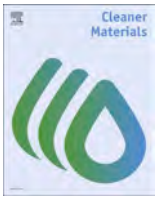

On the feasibility of using Polyester (PE) waste particles from metal coating industry as a secondary raw materials in concrete

Niccolò Aravecchia [a], Jorge Bañuls-Ciscar [b], Alessio Caverzan [c], Giacomo Ceccone [d], Estefania Cuenca [a,*], Liberato Ferrara [a], Konstantinos Grigoriadis [b], Paolo Negro [e], Mattia Rodriquens [a]

[a] Department of Civil and Environmental Engineering, Politecnico di Milano, Italy
[b] European Commission, Joint Research Centre, Directorate for Strategy and Impact, Scientific Development Unit, Brussels, Belgium
[c] European Commission, Joint Research Centre, Directorate for Nuclear Safety and Security, Nuclear Reactor Safety and Emergency Preparedness Unit, Petten, The Netherlands
[d] European Commission, Joint Research Centre, Directorate for Health and Food, Consumer Product Safety Unit, Brussels, Belgium
[e] European Commission, Joint Research Centre, Space, Security and Migration, Safety and Security of Buildings, Ispra, Italy

ARTICLE INFO

Keywords:
Concrete
Polyester
Waste
Secondary raw materials

ABSTRACT

Reduction of CO_2 emissions and plastic waste are the main environmental problems that modern society is dealing with. Concrete industry is continuously investing in research and development aimed at producing sustainable cementitious materials. In the last decades, it has gained interest the possibility of reusing polymer waste (mainly PET or PP) in partial substitution of natural constituents (aggregates) or as fiber reinforcement. As a matter of fact, because of the poor mechanical characteristic of polymers compared to the one of natural aggregates, the final cementitious composite has reduced mechanical performance. In the aforesaid framework, the experimental research reported in this paper aims at verifying the feasibility of a pathway able to use fine polymer particles, in detail a Polyester resin (PE resin) which is a waste product of the coating industry, as a partial replacement of sand and, in case, of binder particles, upon a gamma irradiation process similar to the one used for the sanification of containers in food industry, also their effectiveness in performing as seeds of the cement hydration. Firstly, intrigued by a study performed by MIT researchers (in which exposure of PET waste particles to gamma irradiation has been investigated as a method to improve their mechanical performance), the influence of different gamma irradiation dosages (10 kGy or 100 kGy) on PE resin particles was investigated. However, results led to the conclusion that, even with a mere 5% by volume substitution of Portland Limestone Cement (PLC) in the mix, the process does not significantly improve the mechanical performance of cement-based composites. In a second stage, the non-irradiated particles have been employed as a replacement of the binder and/or of the sand at different volume replacement ratios (10% and 20% respectively) in mortar mix designs formulated from typical Self-Compacting Concrete (SCC) mixes. Finally, once identified the most suitable type and level of replacement as the best compromise between performance maintenance and volume of added particles, the scaling up to the concrete mix-design has been performed and the related performance thoroughly tested. The results have provided limited reduction in mechanical properties, with a 20% by volume level of substitution of cement by PE resin particles, highlighting the possibility of reusing economically viable quantities of PE resins into concrete while still being able to use the material for structural application.

Introduction

Thanks to its economic convenience (low cost) and excellent thermo-mechanical properties including strength, durability, fire resistance and high thermal inertia, concrete is the most widely used construction material and, absolutely speaking, the second most widely used material in the world after water (Schaefer et al., 2018). As a matter of fact, the production of huge quantities of concrete has a strong environmental impact on CO_2 emissions and exploitation of resources. In 2020 the construction industry has accounted for 36% of the global energy

* Corresponding author.
E-mail address: estefania.cuenca@polimi.it (E. Cuenca).

https://doi.org/10.1016/j.clema.2023.100193
Received 21 February 2023; Received in revised form 27 May 2023; Accepted 13 June 2023
Available online 17 June 2023

demand and 37% of energy-related CO_2 emissions (8,7 Giga-tons), 10% of which has been directly produced by the manufacturing of building materials, primarily cement (United Nations, 2021). In detail, for each ton of Ordinary Portland Cement produced, it is estimated that an amount of around 930 kg of CO_2 to be released into the atmosphere (Lehne and Preston, 2018).

Considering that the 2020 world Portland Limestone Cement (PLC) consumption remained at the level of previous year with an amount of more than 4 thousands billion tons used, more than half of which solely in China (2,4 billion tons) (Federbeton, "Rapporto di Filiera, 2020), it is evident that further solutions able to reduce both CO_2 emissions and the quantity of raw materials in cement-based composites without compromising the performance should be sought and implemented. Even before reducing the use of raw materials, since only 50% of CO_2 emissions in Ordinary Portland Cement production is due to direct emission during the oxidation process in the clinker production while 40% is due to fossil fuel combustion products and 10% is due to material transportation, a first solution could be the use of secondary solid fuels in the whole production chain. According to AITEC Sustainability Report (Federbeton, "Rapporto di Sostenibilità, 2020), the use of secondary solid fuels up to 20.9% of the total fuel has led Italian cement manufacturers to reduce emissions at 680 kg of CO_2 per ton of Ordinary Portland Cement, saving 3.0 million tons of CO_2 from 2009 to date.

On the other hand, the high strength-to-weight ratio, lightness, stability over time, resistance to atmospheric agents, impermeability to liquids and gases, electrical and thermal insulation, combined with low production cost, wide availability of raw materials and ease of processing, make polymer-based plastics a versatile material used in the most disparate industrial sectors, from packaging to electronics. It has been estimated that starting form 1950, the annual global production of resins and fibers increased from 2 million tons to 380 million tons in 2015 (Geyer et al., 2017), witnessing an exponential increasing trend in the (single)-use of plastic. Nowadays, the production seems to be stable with 368 million tons produced in 2019, Asia being the first producer with a 51% share, followed by North America and Europe with 19% and 16% respectively (Europe, 2020). Despite the numerous advantages that plastic materials bring to our daily life, there are critical issues related to their management mainly due to the velocity at which polymeric products become waste in relation of their use. The shorter is the life cycle of a product, the higher is its amount as waste. In fact, plastics used in the packaging sector have the shortest life cycle (6 months) and are the most wasted (141 million tons compared to 146 million tons of 2015 annual production). Instead, plastics used in construction sector, which has an average life cycle of 35 years, are among the least wasted (13 million tons compared to 65 million tons of 2015 annual production) (Ritchie and Roser, 2018). This substantial and continuous turnover of materials led the overall production of plastic to amount, up to 2015, to approximately 8.3 billion tons of virgin plastics, 6.3 billion tons of which became waste (Geyer et al., 2017). More specifically, it is the amount of waste produced that raises concern as only 9% and 12% of the worldwide plastic waste produced so far have been properly recycled and incinerated, respectively (Geyer et al., 2017). The rest is stored in landfills or dispersed into the environment, causing an environmental and economic damage (estimated in 13 billion USD annually (United Nations, 2018) since plastic is not biodegradable and often contains additives that extends its break down time up to at least 400 years (Gu and Ozbakkaloglu, 2016). The low percentage in polymers recycling is mainly attributed to high cost. Unlike the storage in landfills, where there is only need of large spaces for waste, incineration or recycling has several critical issues. Although incineration allows to eliminate the greatest amount of solid material, the efficiency of energy recovery is very low. Only about 14–28% of the energy value of incinerated plastic is recovered as electricity, in face of a release into the atmosphere of large quantities of carbon dioxide, harmful gases and toxic residues of combustion in the form of particulate matter as well (Degnan and Shinde, 2019). In the case of recycling, it simply costs much less to get rid of a used product and produce new ones. Recycling process needs intermediate stages, which may be expensive, in which materials are stored, selected, shredded, cleaned, and melted into larger pellets before being reused for a new product. Furthermore, recycling can be complicated by the wide variety of uses, additives and mixtures used in plastic production, which may require different recycling method, by the polymer properties that limit the number of recycling processes (Brooks et al., 2018), or by color change and purity degradation, that reduce the possibility of using recycled plastics in manufacturing new products (Kim et al., 2010).

Because of the above reasons, a synergic solution for reducing the high amount of CO2 emissions and plastic waste as well as depletion of raw materials due to the production of building materials, the use of recycled plastic particles in cement-based materials as plastic fibers or plastic aggregates has been the object of several studies during the last decades. Over the past years, the influence on the material performance has been investigated of several parameters, including type and shape of the polymer employed as recycled constituent in the cementitious composite, replaced natural constituent and relative level of substitution. Among the most widespread polymers listed in Table 1, Polyethylene Terephthalate (PET) is the most used plastic waste in concrete mixes because of its high generated waste-to-produced plastic ratio, low production cost, and its relatively high mechanical properties compared to other polymers.

If used as plastic fibers, plastic wastes are incorporated into the mixture in different shapes (straight, crimped or embossed), sizes and volume percentage to produce fiber-reinforced concrete. Several studies (Kim et al., 2010; Almeshal et al., 2020; Bertolini and Carsana, 2014; Borg et al., 2016; Kim et al., 2008; Foti, 2011; Foti, 2013; Ochi et al., 2007) have demonstrated that this solution brings benefits to cement-based materials improving their toughness and its ability to withstand tensile stresses that may arise from restrained drying shrinkage or thermal deformations. Plastic fibers are able to improve the concrete crack controlling capacity, reduce the formation of internal defects in the material and, with the right geometry, which may also be a characteristic of the product the plastic fibers are "shredded" from, feature quite an efficient bond with the cementitious (Kim et al., 2010; Almeshal et al., 2020; Bertolini and Carsana, 2014). At the same time, the presence of plastic fibers greatly reduces workability, reason why, to guarantee the minimum level of fresh state performance the maximum volume fraction of plastic fibers so far employed in research and application had to be limited to about 1% (Borg et al., 2016; Kim et al., 2008). This fiber content does not significantly alter the mechanical performance of the cementitious composites which, even if both decreased (Kim et al., 2010; Almeshal et al., 2020) or increased (Foti, 2011; Foti, 2013), remains similar to the one of the reference mixture. However, problems may arise because of the long term (in)stability of PET fibers in the concrete alkaline environment, which may result into a worsening of the long term performance due to the creep in cracked concrete (Silva et al., 2005).

When used as plastic aggregates, a higher quantity of plastic waste can be disposed. The polymer particles can replace a percentage of fine aggregate, coarse aggregate or both up to an average of 30% by volume. In this case, most of the studies reported worse mechanical performance in cement-based materials containing plastic aggregates in partial substitution of natural ones, as compared to the reference mixes; this is partially due to increasing in air content and porosity, attributable to the evaporation of excess water in the mixture, due to the impermeability of plastics, that leads to a higher porous macro-structure during aging (Pereira De Oliveira and Castro-Gomes, 2011; Silva et al., 2005) and, in case, to non-homogeneous distribution between natural and plastic aggregates (Albano et al., 2009; Rahmani et al., 2013; del Rey Castillo et al., 2020; Marzouk et al., 2007; Akçaözoğlu et al., 2010; Belmokaddem et al., 2020; Faraj et al., 2019). However, combined with the significantly lower elastic modulus of plastic aggregates than of natural ones, it is the low bond between cement paste and plastic particles

Table 1
Properties, primary production, and waste generation of the most widespread polymers (Ritchie and Roser, 2018; Azhdarpour et al., 2016; Silva et al., 2013).

POLYMER	*ID*	*RECYCLED*	*CATEGORY*	*ρ [Kg/m³]*	*ft [MPa]*	*E [GPa]*	*Production [Million tons]*	*Generated waste [Million tons]*
Polyvinyl chloride	PVC	Occasionally	Thermoplastic	1300–1580	50–60	2.7–3.0	38	15
Polyurethane	PUR	No	Thermosetting	–	–	–	27	16
Polystyrene	PS	No	Thermoplastic	1040–1050	30–55	3.1–3.3	25	17
Polypropylene	PP	Occasionally	Thermoplastic	900–910	25–40	1.3–1.8	68	55
Polyethylene Terephthalate	PET	Yes	Thermoplastic	1270–1390	55–80	2.1–3.1	33	32
Low Density Polyethylene	LDPE	No	Thermoplastic	910–930	8–31	0.2	64	57
High Density Polyethylene	HDPE	Yes	Thermoplastic	950–960	22–31	1.08	52	40
Polyphtalamide	PP&A	Occasionally	Thermoplastic	–	–	–	59	42

surface the main cause of the drop in concrete compressive strength, tensile strength, and elastic modulus. The flat, smooth, and hydrophobic surface of the plastic particles does not allow an adhesion with cement paste to be developed comparable to the one between cement paste and natural aggregates, mainly because of an increase in free water surrounding their waterproof surface and consequently weakening the material micro-structure (Thorneycroft et al., 2018; Umasabor and Daniel, 2020; Akçaözoğlu et al., 2013; Ferreira et al., 2012). However, the use of plastic aggregates brings some benefits especially in concrete failure mechanism. In the case of axial compression, the material can undergo greater deformation before failure occurs (i.e. more ductile) (Albano et al., 2009; Akçaözoğlu et al., 2010; Umasabor and Daniel, 2020; Akçaözoğlu et al., 2013; Sadrmomtazi et al., 2016; Saikia and De Brito, 2014). Slightly different is the behavior of concretes containing plastic aggregate when subjected to flexural loads. Generally, the flexural strength decreases, but in some cases, when the plastic particles have an adequate level of substitution (maximum of 25% by volume of coarse aggregates), shape, size and they are located perpendicular to the cracks, they can improve the strength and toughness providing a "crack-sewing effect" (Silva et al., 2005; Ferreira et al., 2012; Saikia and De Brito, 2014; Frigione, 2010; Hannawi et al., 2010). The partial substitution of natural constituents with plastic aggregates also affects workability, generally resulting into its worsening because of a higher internal friction between the plastic particles and cement paste that hinders the flow and to an amount of water, which, because of surface tension, forms a film around the plastic particles and is thus subtracted from the overall balance in the fluid mixture (Ferreira et al., 2012; Azhdarpour et al., 2016; Basha et al., 2020). However, if very fine and homogeneous particles (Albano et al., 2009) or extruded PET "pellets" (Umasabor and Daniel, 2020; Ferreira et al., 2012) are used, they lead to an increase in workability because of their very smooth surface and almost null water absorption capacity. Even the performance against drying shrinkage worsens when plastic aggregates are used. According to most studies, the greater porosity of the mixture and the lower elastic modulus of both plastic aggregates and concrete itself lead on one hand to a higher shrinkage deformation and on the other to a lower resistance of the material against the internal forces produced by the restrained shrinkage deformation, thus increasing the risk of cracking (del Rey Castillo et al., 2020; Sadrmomtazi et al., 2016; Basha et al., 2020).

Keeping unaltered both the binder content and w/c ratio in the mixtures, all these parameters are equally amplified as the level of replacement, size, and shape heterogeneity of recycled aggregates increase. However, choosing the right aggregates and adopting appropriate correction to the concrete mix design it is possible to control the

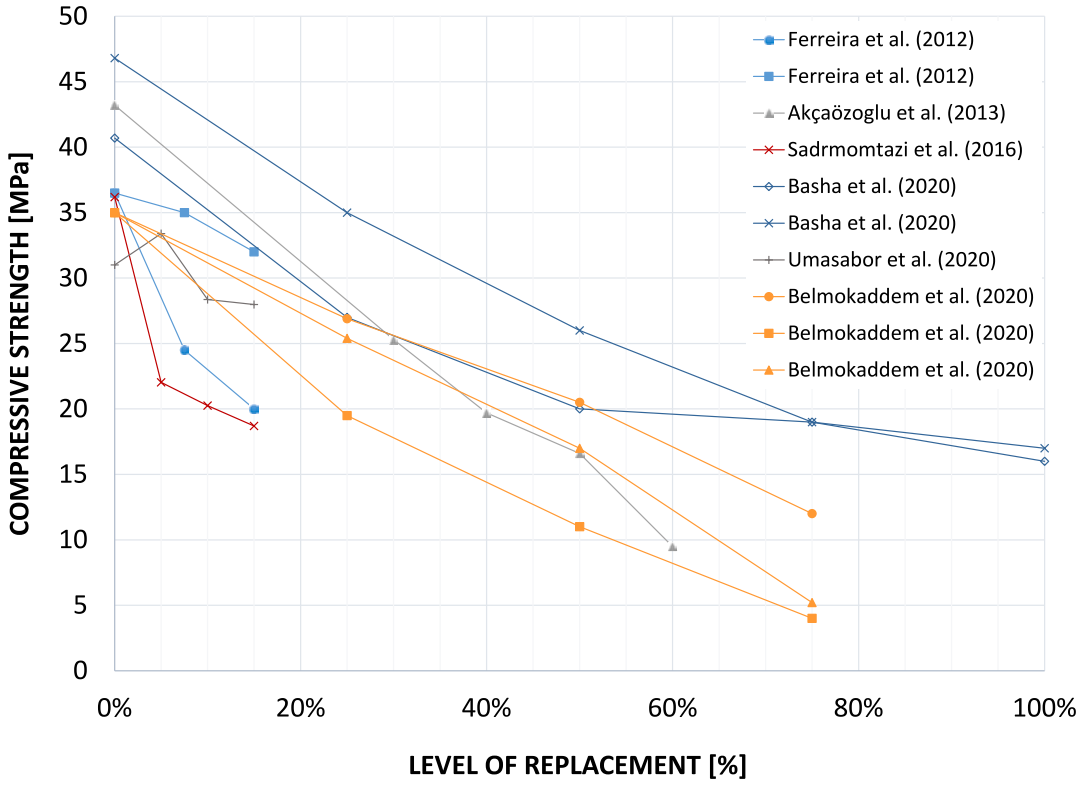

Fig. 1. Influence of the replacement of natural aggregates by recycled plastic particles on the concrete compressive strength.

loss of performance for an effective structural use of the material; investigating the fine aggregate substitution (10% by volume) with PET, it has been ascertained that the more efficient plastic aggregate to be embedded in the mixture must have a rough surface, an irregular shape, must be small enough not to create a dominant breaking surface and with a size comparable to the one of the substituted natural aggregate (Belmokaddem et al., 2020; Ferreira et al., 2012). Fig. 1 shows how the level of replacement of natural fine and coarse aggregates by recycled plastic particles affected the concrete compressive strength based on several recent studies (Belmokaddem et al., 2020; Ferreira et al., 2012).

In this framework, a solution which could lead also to the use of recycled plastic particles as a partial substitution of cement with no detrimental properties on the overall performance of the composite, in case also helping to mitigate the aforesaid negative effects of the use of recycles plastics as replacement of natural aggregates, would be of the foremost importance. A study recently done at MIT (Schaefer et al., 2018) has investigated the gamma irradiation process on PET particles, finding that it increases the degree of crystallinity and chemical bonding of polymer chain which reflects in higher modulus, toughness, stiffness, strength, and hardness of the polymers. This has been claimed to be a possible solution to overcome the drawback of performance loss of the cementitious composite when plastic particles are used as a partial replacement of natural concrete constituents. Utilizing both non-irradiated and irradiated (at two different levels equal to10 kGy and 100 kGy) PET with an average particle size of 170 μm at a 1.25% substitution by dry mass of PLC, the MIT researchers have found an increment in compressive strength equal to 20% in cement paste samples containing 100 KGy irradiated PET as compared to the non-irradiated PET. As a matter of fact, the particles are so fine that they act as hydration seeds since a film of water forms around them promoting the cement hydration.

In this experimental research cement-based materials containing recycled plastic micro-particles have been studied with the principal aim of finding a suitable mix design able to incorporate an adequate quantity of recycled material at the same time minimizing as much as possible the performance reduction of the final material to be still suitable for structural applications. A step-by-step investigation has been performed, producing several mix designs of cement pastes, mortars, and concretes where Polyester (PE) resin particles, waste product of coating industry, are used as replacement of different natural constituents (with particular attention on Ordinary Portland Cement substitution) and at different level of substitution.

First of all, a polymer treatment method should be used that could minimize the material loss of performance when added in the mixture. In view of the promising results obtained in (Schaefer et al., 2018), it has been decided to investigate if gamma irradiation process is effective also for PE resin, testing cement paste and mortar specimens in which 5% by volume of PLC has been replaced by PE resin at the same three irradiation doses chosen by MIT researchers: no Dose, 10 kGy Low Dose, 100 kGy High Dose. Secondly, the effect of the level of substitution of raw materials (i.e. Portland cement and/or sand) by PE resin particles on the physical and mechanical properties of cementitious composites was investigated. To this purpose, mortar specimens have been studied selecting two levels of substitution: 10% and 20% by volume, and investigating three combinations of replaced constituent: replacing only PLC, only sand or both using PE resin as filler at 10% or 20% of the total volume. Only non-irradiated particles have been used, also considering the findings of the previous step. Among all mortar mix designs produced, a specific mix design was identified that can best mediate between a minimum reduction in mechanical performance and an adequate amount of incorporated PE resin particles (20% by volume of PLC). This mix has finally used as starting point of the creation and testing of a concrete mix, evaluating whether it is still suitable for structural uses.

Materials and experimental tests

Polyester resin

The recycled polymer used in this work is a thermosetting Polyester (PE) resin powder, specifically the "PE/P/M BLACK RAL 9005″ provided by "INVER S.p.a" (Fig. 2), waste product of the coating industry. This polymer is widely used thanks to its high resistance against weathering and UV radiation. Specifically, the employed PE resin has a density equal to 1380 Kg/m^3, an average particle size of 3.5 ± 0.4 μm (measured making use of the laser diffraction particle size analyzer "Mastersizer 3000® Malvern®") and a contact angle θ equal to 74.4° ± 5.0°, characterizing polyester resin as a hydrophilic material. The chemical composition of PE resin has been investigated through both X-ray photoelectron spectroscopy (XPS) and Energy-Dispersive X-Ray spectroscopy (EDS) analysis, identifying Carbon, Oxygen and Calcium as principal constituents, which could make PE resin a good material interacting with Ordinary Portland Cement and not just an inert aggregate.

The PE resin employed in the first stage of the research was irradiated in an irradiation facility "Gammatom S.r.L" constituted by 140 Cobalt-60 rods for an overall capacity of 800 KCi (Ci = Curie unit). The PE resin has been gamma irradiated at the two dosages of 10 KGy with one single irradiation cycle and 100KGy with four irradiation cycles each of them with a 25KGy dosage.

Mix designs

Table 2 and Table 3 show the mix designs of cement pastes and mortars both without PE resin and with 5% by volume of PLC substituted by PE resin at the three different irradiation doses that were cast to assess if the gamma irradiation process on PE resin can partially recover the mechanical properties of cement-based materials incorporating PE particles. The specimens were cast using a limestone Portland Cement type CEM II/A-LL 42,5 R and, in the case of mortar, a siliceous sand with a maximum aggregate size of 4 mm and a fineness modulus of 2,83 was employed. The mix composition was always adjusted to keep the water/cement ratio unaltered to 0,5.

The same type of "raw" constituents were used to cast the mortar specimens tested to investigate the influence on the mechanical and physical properties of the level of substitution and the type of natural constituent substituted. The mix designs obtained imposing the 10% or 20% by volume substitution of PLC only, sand only or using PE resin are reported in Table 4. Only non-irradiated PE particles were used, also considering the findings of the previous step. When PE resin replaced PLC, the mix composition was adjusted to maintain the w/c ratio unaltered to 0,5. In the case of PE resin used as filler at 20% of the total volume, the superplasticizer DYNAMON NRG 1022 was added into the mix (1% of cement mass) to guarantee the level of fresh state performance necessary to cast the specimens.

Finally, to cast concrete specimens, Portland limestone cement CEM II/A-L 42,5 R was used with siliceous sand up to 4 mm with fineness modulus equal to 3.67 and two different types of gravel: one characterized by grain dimensions between 6 mm and 10 mm with fineness modulus equal to 5.85 and the other characterized by grains dimension between 8 mm and 20 mm with a fineness modulus equal to 7.24. Based on the experimental results of mortar, the 20% substitution by volume of PLC with PE resin has been considered the best combination in term of performance reduction and amount of PE resin incorporated in the mixture. Therefore, it has then been utilized for implementing the scale up to concrete mix design which is shown in Table 5. Moreover, Table 6 includes the granulometric size distribution of the natural aggregates (sand and gravel) used in the mixes.

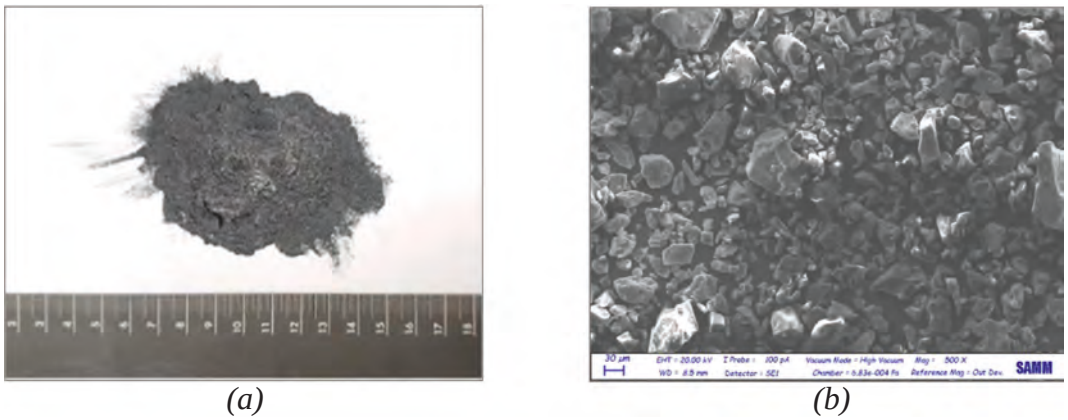

Fig. 2. Polyester resin (a) and its SEM image (b).

Table 2
Cement paste mix designs having PE resin at different irradiation doses. "P"=cement paste, "X-PL"=percentage substitution by volume of PLC, "ND"=No irradiation, "LD"=Low dose 10KGy, "HD"=High Dose 100KGy.

		P-0%-PL	*P-5%-PL-ND*	*P-5%-PL-LD*	*P-5%-PL-HD*
w/c ratio	–	0.5	0.5	0.5	0.5
CEM II A-LL 42.5 R	[Kg/m^3]	1216	1191	1191	1191
Water	[Kg/m^3]	608	595.5	595.5	595.5
PE resin	[Kg/m^3]	–	27.9	27.9	27.9

Table 3
Mortar mix designs having PE resin at different irradiation doses. "M"=mortar, "X-PL"=percentage substitution by volume of PLC, "ND"=No irradiation, "LD"=Low dose 10KGy, "HD"=High Dose 100KGy.

		M−0%-PL	*M−5%-PL-ND*	*M−5%-PL-LD*	*M−5%-PL-HD*
w/c ratio	–	0.5	0.5	0.5	0.5
CEM II A-LL 42.5 R	[Kg/m^3]	602	590	590	590
Water	[Kg/m^3]	301	295	295	295
Sand	[Kg/m^3]	1362	1362	1362	1362
PE resin	[Kg/m^3]	–	13.8	13.8	13.8

Specimens casting and curing process

All the cement paste and mortar mixes and specimens (72 cement paste prismatic specimens and 180 mortar prismatic specimens) were realized following the steps indicated by the Standard UNI EN 196-3 and UNI EN 196-1 respectively. In a casting room where temperature and relative humidity are constant to 20 ± 2 °C and 65% RH, the mixing process was done making use of a 5 L capacity mixing machine manufactured by "CONTROLS S.p.a.". Once the mixing process had been completed, the mixture was cast in a steel mould consisting of three identical 160x40x40 mm compartments, previously oiled for a better demoulding and firmly clamped to a jolting apparatus used for compacting the mixture. Each mould was filled in two steps each of one consisting in half filling the mould and compacting the mixture with 60 jolts. For the specimens earmarked for shrinkage evaluation, stainless steel measurement studs were preinserted, that will follow the specimen in its shrinking deformation allowing the shrinkage measurement. Right after the casting, the moulds were covered by a glass plate and stored in a climate room in which temperature and relative humidity are constantly maintained to 20 ± 2 °C and 90% RH. After 24 h, specimens were demoulded. The specimens for mechanical tests were put back in the same climate room for the prescribed curing period (3, 7, 28 and 56 days), while the specimens used for shrinkage evaluation were moved in a different climate room in which temperature and relative humidity are constant to 20 ± 2 °C and 50% RH and stored until the stabilization of the shrinkage value.

Concrete specimens were cast following the prescription given by the standard EN 12350-1, making use of the TTM140 mixing machine purchased by SIPE. It has been followed the same casting and curing

Table 5
Reference concrete mix design and mix design having 20% substitution by volume of PLC.

		REF	*C-20%-PL*
w/c ratio	–	0.5	0.5
CEM II A-L 42.5 R	[Kg/m^3]	360	332
Water	[Kg/m^3]	180	166
Sand	[Kg/m^3]	814	814
Gravel	[Kg/m^3]	1077	1077
Super plasticizer	[Kg/m^3]	2.2	2.0
PE resin	[Kg/m^3]	–	36.9

Table 4
Mortar mix designs having different replaced natural constituents. "M"=mortar, "X-PL"=percentage substitution by volume of PLC, "X-SAND"=percentage substitution by volume of sand, "X-FILLER"=percentage of total volume replaced by PE filler.

	M−0%-PL	*M−10%-PL*	*M−20%-PL*	*M−10%-SAND*	*M−20%-SAND*	*M−10%-FILLER*	*M−20%-FILLER*
w/c ratio	0.5	0.5	0.5	0.5	0.5	0.5	0.5
CEM II A-LL 42.5 R [Kg/m^3]	602	577	548	602	602	542	482
Water [Kg/m^3]	301	288.5	274	301	301	271	241
Sand [Kg/m^3]	1362	1362	1362	1226	1090	1226	1090
Super plasticizer [Kg/m^3]	–	–	–	–	–	–	4.8
PE resin [Kg/m^3]	–	28.5	61.1	69.6	139.2	138.0	276.0

Table 6
Granulometric size distribution of the natural aggregates.

Sand Diameter (mm)	Passing (%)	Gravel Diameter (mm)	Passing (%)
0.063	0.065	2.5	0
0.08	0.584	3.15	0.809
0.1	5.253	4	3.045
0.125	5.901	5	10.365
0.16	7.004	6.3	19.779
0.2	7.977	8	27.897
0.25	9.144	10	38.815
0.315	10.506	12.5	63.064
0.4	12.192	14	72.878
0.5	14.332	16	86.665
0.63	17.575	18	95.654
0.8	20.169	20	99.922
1	23.735		
1.25	28.470		
1.6	33.917		
2	64.202		
2.5	91.569		
3.15	97.665		
4	99.870		
5	100		
6	100		
8	100		
10	100		

procedure described for cement pastes and mortars with differences in molds dimensions and vibrating mode. It was used a total of 18 cubic moulds with 100 mm side and 6 with 150 mm side, 18 cylindrical moulds (φ = 100 mm, h = 300 mm) and 24 prismatic moulds (100x100x500 mm). Once totally filled with the mixture, the moulds were placed on a vibrating table to compact the mixture vibrating the moulds for few seconds.

Mechanical and physical tests

Mini-Slump test

Mini-Slump test is the principal method for determining the consistence of freshly mixed mortar and cement pastes. Executed twice for each cement paste and mortar mix, the test was performed following the standard procedure required by UNI EN 1015-3. The reported flow value is the average between the measurements done in the two tests.

Efflux test

To determine the fluidity of freshly mixed cement paste, efflux test has been performed on the four different cement paste mixes following the procedure prescribed by UNI EN 445:2007 and ASTM C939/C939M employing the Marsh cone test. The fluidity is measured by the time for a given amount of fluid mixture to flow out of the cone, equipped with a 10 mm diameter outlet nozzle.

Setting time test

Initial and final setting times of cement paste samples were determined through the Vicat test using the Vicat apparatus purchased from RMU Testing Equipment S.R.L and choosing a step of 10 min as time interval between two measurements. Differently from what is prescribed by the Standard UNI EN 196-3, the test has been performed in a climate room having relative humidity of 90% RH and the mould was not immersed in water.

Rheometry tests

In case of concrete, a more quantitative estimation of fresh-state properties can be derived through rheometric test in terms of fundamental physical quantities, such as plastic viscosity μ and yield stress $\tau 0$, under the assumption the fresh concrete behaves like a Bingham fluid. In this work, these parameters were measured making use of the ICAR Plus Concrete Rheometer, purchased from "Germann Instruments". It consists of a 20 L container having an inner radius equal to 305 mm in which concrete is placed, and in a multi-blade vane (φ = 127 mm, h = 127 mm) assembled on a motor drive/torque meter unit. Two different tests can be performed. Applying a constant vane speed (0.025 rad/s) and measuring the torque necessary to maintain such velocity, the stress growth test determines the static yield stress τ_0, in MPa, as a function of the peak torque T in Nm, the vane diameter D and vane height H, both in mm, as indicated by equation (1):

$$\tau_0 = \frac{2 \bullet T}{\pi \bullet D^3 \left(\frac{H}{D} + \frac{1}{3}\right)} \tag{1}$$

The flow curve test computes the Bingham parameters of dynamic yield stress $\tau 0$ and plastic viscosity μ. Imposing to the vane an initial rotation speed of 0.5 rad/s, a final one of 0.05 rad/s and the number of steps, it is possible to create a torque-speed curve interpolating the obtained value. Depending on the rotation speed Ω [rad/s], the torque T [Nm], the vane height h [mm], the vane radius $R1$ [mm] and the outer container radius $R2$ [mm], the Bingham parameters are automatically computed by the software on the base of the Reiner-Rivlin equation (2):

$$\Omega = \frac{T}{4\pi h \mu}\left(\frac{1}{R_1^2} - \frac{1}{R_2^2}\right) - \frac{\tau_0}{\mu} ln\left(\frac{R_2}{R_1}\right) \tag{2}$$

Flexural test

For cement paste and mortar specimens, the flexural strength was measured following the prescription of UNI EN 1015-11. By means of a METRO COM testing machine set to a loading rate of 5 Kg/s, a three-point bending test was performed on 160x40x40 mm specimens up to failure at 24 h, 3 days, 7 days, 28 days and 56 days of curing. At each considered curing age, three nominally identical tests were performed; the arithmetic average of the individual values and the standard deviation σ of was then computed. Converting the failure load P from Kg to N and, considering both the cross-section of the specimens ($b = d = 40$ mm) and the distance between the supporting rollers ($l = 106.7$ mm), the flexural strength $f_{ct,fl}$ has been evaluated, in MPa, as indicated by equation (3):

$$f_{ct,fl} = \frac{3}{2}\frac{P \bullet l}{b \bullet d^2} \tag{3}$$

In case of concrete specimens, the flexural strength was determined following the prescription of UNI EN 12390-5. The flexural strength was evaluated only at a curing age of 7, 28 and 56 days performing three nominally identical tests at each curing age as before and computing then the arithmetic average of the individual values and the standard deviation σ. The three-point bending tests on concrete specimens were carried out on an INSTRON testing machine with a100 kN maximum capacity. 500x100x100 mm prismatic specimens previously notched in the middle creating a 10 mm deep notch were tested up to failure. The notch allowed the measurement the crack mouth opening displacement (CMOD) which permits to evaluate the fracture energy of the specimen. The tests were performed in CMOD control set to 0.05 μm/s. The failure load P was recorded by the machine in Newtons and CMOD was measured by a clip gauge in microns. The flexural strength $f_{ct,fl}$ was evaluated in MPa using the previous Equation (3) considering the reduced cross-section ($b = 100$ mm, $d = 90$ mm) and the distance between the supporting rollers ($l = 450$ mm).

Compressive test

For cement paste and mortar, following again UNI EN 1015-11, the compressive strength test was carried out on halves of the specimens previously broken in flexure. Consequently, considering each mix design, six half specimens were tested at each selected curing age (24 h, 3 days, 7 days, 28 days, 56 days) and the arithmetic average of the individual values and the standard deviation σ were computed. Compressive tests were performed by means of a METRO COM testing machine set to a loading rate of 40 Kg/s. Converting the failure load P

from Kg to N and, considering the cross-section of the specimens ($b = d = 40$ mm), the compressive strength fc has been evaluated, in MPa, as indicated by equation (4):

$$f_c = \frac{P}{b \bullet d} \tag{4}$$

Concrete compressive strength tests were carried out, following the Standard UNI EN 12390-3, testing three 100 mm cubic samples at each different curing age of 24 h, 3 days, 7 days, 28 days and 56 days. Moreover, three 150 mm cubic samples were tested at 28 days, while at 7, 28 and 56 days of curing three cylindrical samples previously subjected to elastic modulus test were further. At each specific curing age, both the final cubical and cylindrical compressive strength of each mix design have been evaluated as the arithmetic average of all the individual values and the related standard deviation σ was calculated as well. Compressive tests were performed making use of two different testing machine, one for cubic sample and one for cylindrical sample, both purchased from "CONTROLS S.p.a." which work in load control set to 1 MPa/s, recording the failure load P [N] of the specimens. As a function of the cross-section dimension b [mm] and d [mm] or the diameter D [mm], the cubic compressive strength Rc and cylindrical compressive strength fc were evaluated in MPa respectively by equations (5) and (6):

$$R_c = \frac{P}{b \bullet d} \tag{5}$$

$$f_c = \frac{P}{\pi \bullet \frac{D^2}{4}} \tag{6}$$

Elastic modulus evaluation

Evaluated only for concrete, the secant modulus of elasticity in compression was determined according to UNI EN 12390-13. For each mix design, three cylindrical specimens (φ = 100 mm, h = 300 mm) underwent three axial compressive loading cycles imposing a loading and unloading stress rate set to 0.6 MPa/s up to a maximum stress level equal to one-third of compressive strength. Placed symmetrically with respect to the central axis of the specimen, each of that at a height between two-thirds of the specimen diameter and one-half of the total height, three DD1 displacement transducers measured the specimen deformation then used to evaluate the strain as the ratio between the average measured deformation and the gauge length. Considering the maximum stress level σ_a [MPa], the initial stress of the third cycle σ_p [MPa], the strain at the end of the loading phase in the third cycle ε_a and the strain at the end of the unloading phase in the second cycle ε_p, the stabilized secant modulus of elasticity $E_{c,s}$ was evaluated in MPa as indicated by equation (7):

$$E_{c,s} = \frac{\sigma_a - \sigma_p}{\varepsilon_a - \varepsilon_p} \tag{7}$$

Shrinkage evaluation

Shrinkage is the unrestrained linear movement arising from drying condition of cement-based materials and it is the sum of the autogenous shrinkage and the drying shrinkage. In the case of cement paste and mortar its determination was performed according to UNI EN 12617-4 on three standard 160x40x40 mm specimens evaluating the final shrinkage strain as the average of these three individual values. Placed in the same climate room where the specimens are curing (T = 20 °C, R. H = 50%), the length variation measuring apparatus is composed by an iron shell on which is fixed a digital micrometer dial gauge having an accuracy of ± 0.001 mm. Considering an initial length L equal to 160 mm and measuring ΔL [mm] as the difference between the reading in the measurement apparatus taken at the demoulding and the reading in the measurement apparatus taken at a generic curing age, the shrinkage strain is expressed in mm/m as indicated by equation (8):

$$\varepsilon = 1000 \frac{\Delta L}{L} \tag{8}$$

UNI EN 12617-4 advises to also measure the mass variation of cement paste and mortar specimens during the curing age due to water loss. With the use of a scale, the specimens have been weighed to the nearest 0,1 g. Again, for each mix design, measurements on three nominally identical specimens were performed evaluating the final mass variation as the average of the individual values. Considering as reference the mass measured after the demoulding M_0 [g], the specific mass percentage variation m has been determined as follow in equation (9):

$$m = 1000 \frac{\Delta M}{M_0} \tag{9}$$

In case of concrete, shrinkage deformation was determined according to UNI EN 12390-16 on three 500x100x100 mm prismatic specimens, evaluating the final deformation as the average of these three values. The shrinkage strain has been calculated following Equation (8), considering an initial length L of 500 mm.

Calorimetric test

Calorimetric test was performed on mortar samples according to UNI EN 12390-15 by means of the adiabatic calorimeter 54-C2010/A purchased by "CONTROLS S.p.a.". It is an adiabatic method that allows to determine the temperature reached and the heat released during the hardening process.

Fluorescence analysis

A fluorescent microscope (Zeiss Axio Imager M2) was used to assess the spatial distribution of PE resin particles over mortar samples. Samples fractured cross-section were imaged using an irradiation source with a wavelength set to 615–648 nm. 384 tiles were acquired using a Axioncam 512 imaging device and an objective EC Plan-Neofluar 5x generating a final image with dimensions equal to 42,14 × 42,14 mm^2 and resolution of 22656 × 22656 pixels.

Thermo-gravimetric (TGA) analysis

TGA analysis determines thermal stability and fraction of volatile components of a material by monitoring the weight change that occurs as the material (mortar in this case) sample is heated at a constant rate. In this case, the measurement was carried out to obtain information about chemical phenomena of thermal decomposition. TGA was performed on a 100 mg mortar sample, previously shattered into powder, using the "Ta Instrument Q500″ analyzer setting a thermal rate of 30 °C/min up to 900 °C and a nitrogen flux of 25 ml/min.

Mercury intrusion porosimetry (MIP) analysis

MIP analysis was performed on cement paste samples to measure the pores size distribution of the different samples at curing ages of 3, 7 and 28 days, utilizing the AutoPore IV 9500 V1.07 purchased from "Micrometrics Instrument Corp.". MIP analysis consists in applying a controlled, progressively higher external pressure and then measuring the volume of mercury that intrudes into the sample. From the pressure value, it is possible to obtain the pore size distribution using the Washburn equation (10). Assuming the pore as a cylinder, its diameter D is found imposing the equilibrium between penetration resisting force f_R, which depends on mercury surface tension γ and contact angle θ, and the external force produced by the vacuum f_{Ext}, which depends on the imposed pressure P.

$$f_R = \pi D \gamma cos\theta; ; f_{Ext} = PA = \frac{P\pi D^2}{4} \Rightarrow D = \frac{4\gamma cos[03B8]}{P} \tag{10}$$

Scanning electronic microscope (SEM) analysis

SEM analysis was performed on mortars to highlights the cement matrix-PE resin interface, investigating if the presence of PE resin

produces a weakening in the bonding with respect to a traditional cement paste.

Results and discussion

Influence of gamma irradiated PE resin

Efflux test

The measured efflux times of cement pastes have been reported in Fig. 3. PE resin used as 5% substitution by volume of Portland limestone cement results into an increment in viscosity of all the cement pastes tested. A significant difference in efflux time is visible between non-irradiated particles (+3.1% compared to reference) and irradiated particles, the effects appear to be insensitive to the irradiation doses (+15.3% for 10 kGy, +16.0% for 100 kGy). A hypothesis for which mixes containing irradiated PE resin particles have higher viscosity can be identified in the gamma irradiation process that may have modified the particle surface in such a way to produce a higher friction in the mixture between them and cement paste, thus hindering the flowing through the Marsh cone nozzle. Furthermore, a higher chemical compatibility between particles that may even cause the faster creation of particles clusters, as hypothesized in (Schaefer et al., 2018).

Mini-Slump test

The slump-flow values obtained for cement paste mixes (Fig. 4-a) show that, regardless the irradiation dose, all the mixes in which PLC is substituted at 5% by volume with PE resin undergo a similar reduction in workability, featuring a percentage reduction with respect reference mix equal to −6.9% for P-5%-PL-ND, −10.4% for P-5%-PL-LD and −5.7% for P-5%-PL-HD. Even if limited, the reduction in workability consequent to the addition of PE resin can be mainly explained by the high finesses and specific surface of PE particles that, being surrounded by a film of water because of surface tension, subtracts to the mixture a high amount of water.

Even in the case of mortar mixes, the flow values reported in Fig. 4-b show that 5% substitution by volume of PLC with PE resin results into a decrease in workability, which is scantly affected by the different irradiation doses. With respect to the reference mix, the percentage reductions, whose causes are the same as those mentioned above, are quite negligible and similar to those already measured for the cement pastes, in detail equal to −5.8% for M−5%-PL-ND, −7.2% for M−5%-PL-LD and −3.7% for M−5%-PL-HD. Nevertheless, when PE resin were irradiated with the maximum dosage 100KGy (HD) the reduction in workability was slightly lower compared to the values obtained for low irradiation (LD) and no irradiation (ND).

Flexural strength test

The obtained flexural strength values of the cement paste specimens (Fig. 5-a) show that 5% replacement by volume of PLC with PE resin irradiated at the three different doses affects the results in an unstable way. For early to intermediate curing ages no significant variations in terms of flexural strength have been observed (only the specimens with non-irradiated PE resin particles featured at 3 days a higher strength). Neglecting the experimental outlier of the reference mix at 28 days that reached an early collapse with a relatively low flexural strength, at later ages a reduction in strength can be recognized when the polymer particles are added, basically irrespective of the irradiation doses (-26.53% for P-5%-PL-ND, −17.74% for P-5%-PL-LD, −18.21% for P-5%-PL-HD at 56 days). This could be due to the quality of the interface which may be more porous in the long term, likely because of the film of water adsorbed on the resin particle surface.

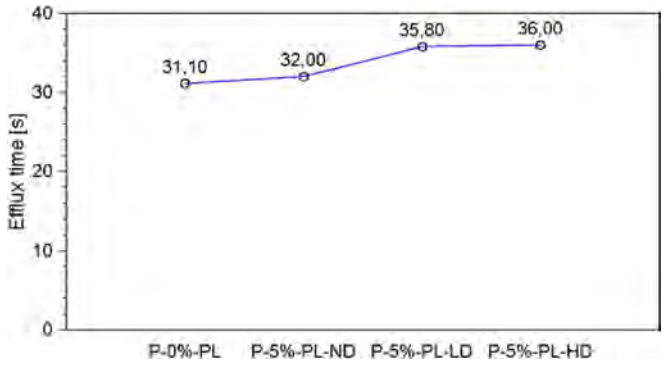

Fig. 3. Efflux time in cement pastes containing PE resin at different irradiation doses.

In case of mortar specimens having 5% substitution by volume of PLC with PE resin particles irradiated at different doses, the flexural strength results reported in Fig. 5-b are quite homogeneous during curing. At 1 days, the maximum flexural strength variation equal to −2.23% for the specimens having low irradiated particles shows the negligible influences of PE resin on the early-stage resistance. Starting from 3 days of curing, higher variations start being recorded, in any case limited to 1 MPa (around 15%), which fluctuate according to the different irradiation doses. At 28 days of curing, the percentage variations have been evaluated equal to −7.94% for M−5%-PL-ND, +3.85% for M−5%-PL-LD and + 1.61% for M−5%-PL-HD. Values at 56 days of curing show that the presence of PE resin in the mixes results into a decrease in flexural strength as already detected with reference to paste specimens, such a reduction increasing with the increasing irradiation dose.

Compressive strength test

Fig. 6-a shows the obtained compressive strength of the cement paste specimens cast employing a 5% substitution by volume of PLC with gamma irradiated PE resin particles at different doses. Apart from 7 days of curing, where compressive strength is the highest in reference mix, while for mixes containing PE resin it decreases with the increasing of the irradiation dose, the data of the remaining curing ages show very similar compressive strength values for all the mixes, regardless of the different PE resin irradiation doses. With respect to reference mix, the compressive strength variation at 28 days of curing has been found equal to −0.12% for P-5%-PL-ND, +2.93% for P-5%-PL-LD and + 2.54% for P-5%-PL-HD.

The obtained average compressive strength values of mortars (Fig. 6-b) show how the addition of PE resin determines almost constant effects on all the different tested mixtures at each considered curing age. Unlike all the curing ages where the percentage variation of compressive strength with respect to the reference is between −3% and + 5%, at 3 days it has been found the highest variation in strength among all the mixes. The reference mix has the highest compressive strength, while the lowest has been developed by the mix having 100 kGy high irradiated PE resin (-9.19%). The strength of the other two mixes having non-irradiated and 10 kGy low irradiated particles can be considered comparable to the reference one (-4,89% and −2.13% respectively).

Shrinkage deformation and mass variation

Fig. 7 shows the evolution of the drying shrinkage deformation in cement paste specimens cast substituting 5% by volume of PLC with PE resin at three different irradiation doses. Shrinkage deformation is very similar in all the mixes, only a slightly higher deformation for mixes containing PE resin was observed that, anyway is not influenced by the irradiation dose of the plastic particles. At stabilization (83 days), the percentage variation of shrinkage deformation compared to the reference have been evaluated as: +2.58% in P-5%-PL-ND, +4.43% in P-5%-PL-LD and + 3.43% in P-5%-PL-HD, deducing that PE resin incorporation is irrelevant for this property.

In case of mortar specimens having 5% by volume of PLC substituted with PE resin particles irradiated at different doses, the evolution of shrinkage deformation (Fig. 8-a) shows that the mixtures containing PE

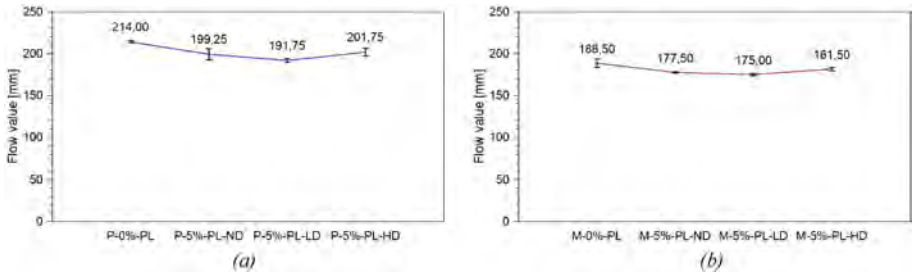

Fig. 4. Flow value for cement pastes (a) and mortars (b) containing PE resin at different irradiation doses.

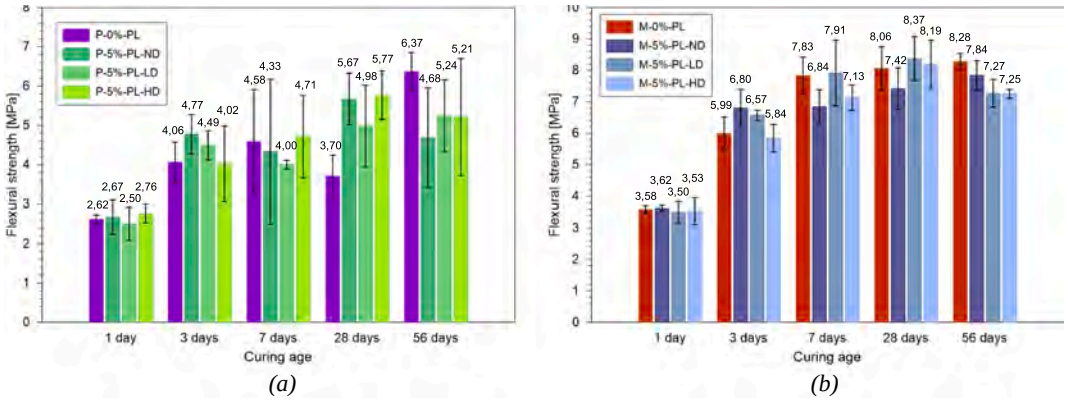

Fig. 5. Flexural strength for cement pastes (a) and mortars (b) containing PE resin at different irradiation doses.

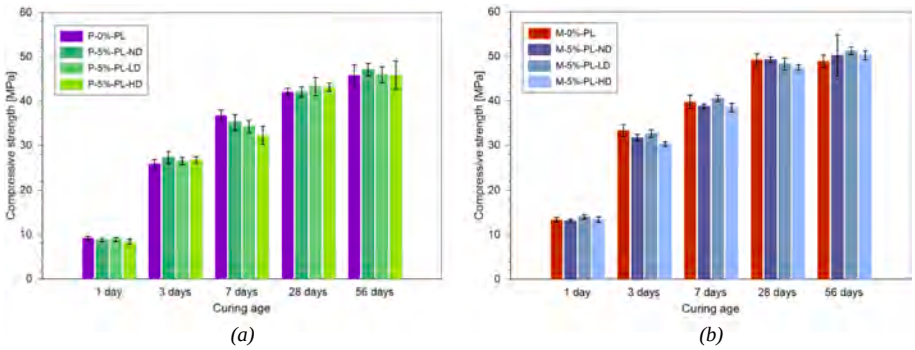

Fig. 6. Compressive strength for cement pastes (a) and mortars (b) containing PE resin at different irradiation doses.

resin underwent to a lower shrinkage deformation than reference mix, which remains almost constant among the different irradiation doses. The percentage variation at stabilization (83 days) is equal to −5.21% in M−5%-PL-ND, −5.16% in M−5%-PL-LD and −7.51% in M−5%-PL-HD, mainly due to the lower amount of water able to evaporate from the mixtures. From these results, it can be said that 5% substitution of PLC with PE resin brings to a quite negligible reduction in shrinkage deformation, which is also not affected by the different irradiation dose of particles used. Mass variation (Fig. 8-b) is coherent with the shrinkage evaluation and so it is affected neither by the presence of PE resin nor by its irradiation dose. The mass variation stabilized at −5.91% for M−0%-PL, −5.77% for M−5%-PL-ND, −5.76% for M−5%-PL-LD and −5.79% for M−5%-PL-HD, showing that the addition of PE resin does not affect this value.

Influences of level of substitution and substituted constituent

In the following, when reference is made to the results about PLC substitution, all the results concerning M−5%-PL are the same of the specimens M−5%-PL-ND of the previous Section 3.1. They have been added in the discussion for sake of completeness.

Mini-Slump test

The values of the slump flow diameters for mortar mixes having the three different combinations of replaced constituent are reported in Fig. 9 as function of the level of substitution.

When PE resin particles substitute part of the PLC, compared to the reference mix, the reduction of the flow value has been calculated equal to −5.8% for the 5% substitution, −10.2% for the 10% substitution, –22.6% for the 20% substitution, with a percentage loss of workability assumable directly proportional to the PE resin level of replacement.

In the case of partial sand substitution, the reduction of flow value with respect to the reference mix has been calculated equal to −0.9% and −6.9% respectively for the 10% and 20% substitution.

The highest reduction in flow value has been recorded when PE resin particles was used as filler of a total volume percentage. The reduction of workability with respect to the reference mix has been calculated equal to −26.1% for the 10% substitution, −42.9% for the 20% substitution.

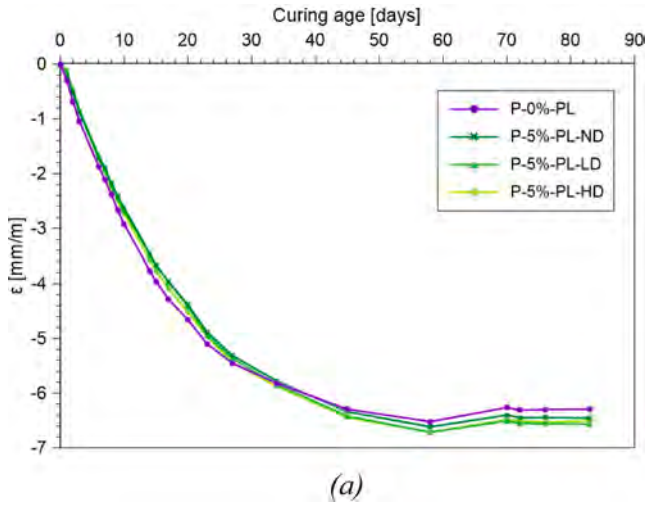

Fig. 7. Shrinkage deformation for cement pastes containing PE resin at different irradiation doses.

The first aspect that could explain the reduction in workability, which increases approximately linearly as the level of substitution increases, is the different amount of water in the mixture. Except for the mix design in which PE resin substitutes part of the sand, all the other mixes contain less water than the reference one. The other reason could be identified in the hydrophilicity and high specific surface of PE resin which, during the mixing process, subtracts to the mixture more water than the substituted constituents making it more viscous. Analyzing the results, since the mixes in which PE resin particles partially replace sand featured the lowest decrease in workability, a sort of lubricating effect of the former on the second can be likely hypothesized, the nature and shape of the particles justifying the assumption.

Setting time test

As shown in Fig. 10, PE resin particles in substitution of Portland limestone cement do not bring to significant variations in initial and final setting time at any level of substitution. Apart from the cement paste sample having 5% substitution by volume of Portland limestone cement for which an initial time of 380 min was recorded, all the other samples featured a similar value between 400 and 410 min. Instead, it was not possible to identify the exact value of final setting time since the 0,5 mm needle penetration value given by the standard is of a too high precision for the adopted measurement equipment. However, it is recognizable for all the specimens a similar trend in which after 700 min the needle penetration is lower than 1 mm, this limit having been reached with a slight decreasing setting rate as the level of substitution increases. Interesting is the result obtained for 5% replacement by volume of Portland limestone cement from which it can be hypothesized that PE resin provokes a seed effect in the cement hydration process which is accelerated. This effect then vanishes when the level of substitution increases since its benefit is balanced by the lower content of cement in the mixtures.

Flexural strength test

Fig. 11-a reports the values of the flexural strength obtained in the case in which PE particles have been employed as partial replacement of the PLC. At the different curing ages, the different level of PE resin particles replaced in the mixes affects the results in a rather random way, making it impossible to identify a trend between level of substitution and strength variation. Considering the average value, at 24 h and 3 days the variation in strength can be considered negligible for all the three levels of substitution with a peculiarity in the M−5%-PL mix whose flexural strength at 3 days is the highest (+13.52% compared to the reference). Starting from 7 days of curing, the reference mix becomes the one with the highest strength while the other mixes containing PE resin undergo a decrease in strength with a maximum variation of −16.80% for M−10%-PL at 7 days. Looking at the early-stage values, it can be noticeable again that PE particles may create a seed effect on the cement hydration, an assumption which, already corroborated by the setting time results above, is also confirmed by the fact that at constant w/c

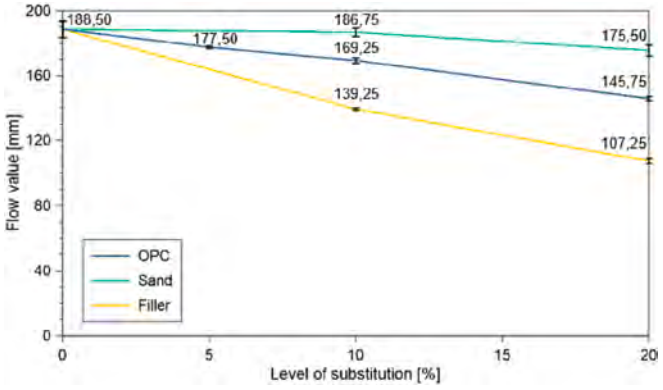

Fig. 9. Flow value for mortars containing PE resin at different levels of substitution and substituted fferent constituents.

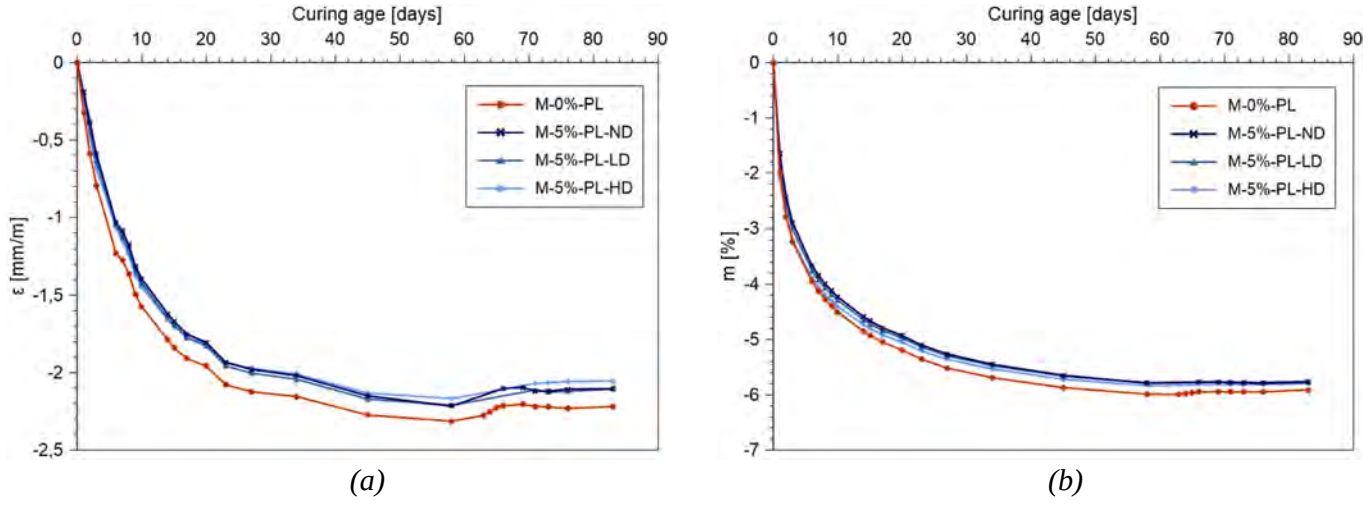

Fig. 8. Shrinkage deformation (a) and mass variation (b) for mortars containing PE resin at different irradiation doses.

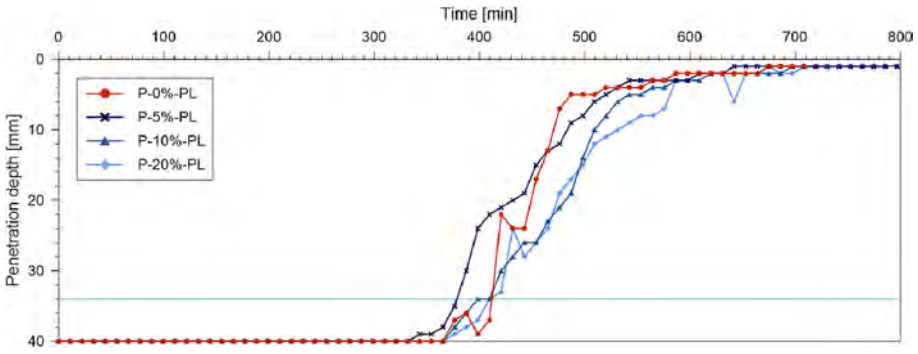

Fig. 10. Setting times for PLC substitution at different levels of substitution.

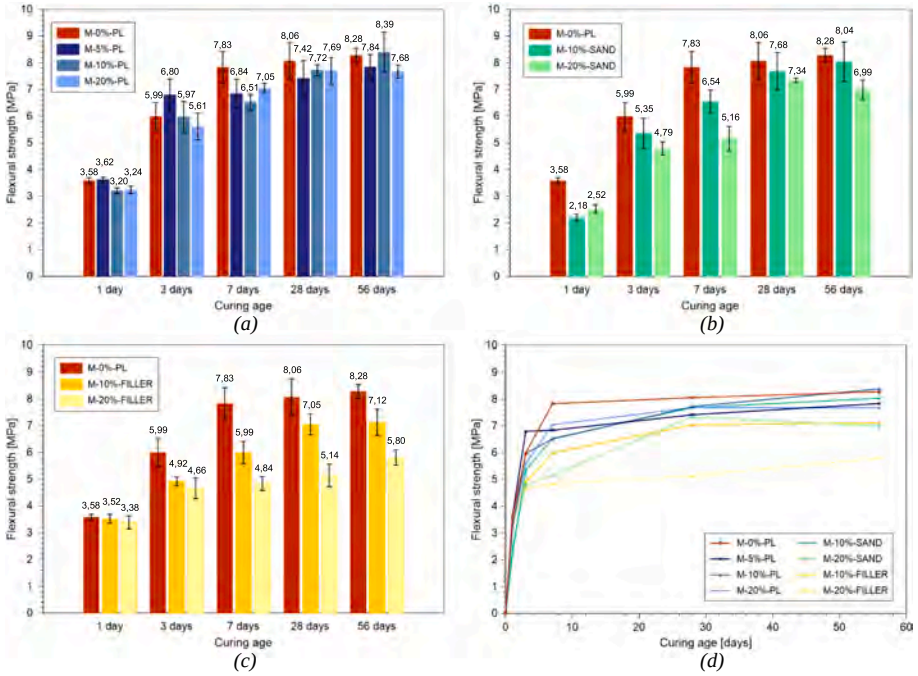

Fig. 11. Flexural strength for mortars having PLC substitution (a), sand substitution (b) or PE used as filler (c) at different levels of substitution and global superimposing of results (d).

ratio but with a decreasing absolute content of cement the variations in flexural strength are well below 10% (except for 7 days where it is a little higher).

When PE resin partially substitutes the sand, the flexural strength values reported in Fig. 11-b highlight a more significant reduction in flexural strength. The main cause is likely the missing toughening effect of the coarser sand grains. Except for the evaluation after 24 h, among the mixes having recycled particles, the flexural resistance of M−10%-SAND is always higher than M−20%-SAND with a percentage reduction that is about the half. At 28 and 56 days, the flexural strength of M−10%-SAND and M−20%-SAND tend to be recovered computing, at 28 days, a percentage variation equal to −4.67% and −8.93% respectively, hypothesizing a possible delay in the hydration of cement due to the presence of PE resin which slowly release the water surrounding its surface.

When PE resin was employed as filler, Fig. 11-c shows that at 24 h, flexural strength has no significant variation among the mixes and that the seed effect on cement hydration is still visible, while starting from 3 days of curing the reference mix is the one with the highest strength. At 28 days, M−10%-FILLER and M−20%-FILLER mixes perform a flexural strength which has a percentage reduction equal to −12.58% and −36.21% respectively. The marked reduction obtained for the specimen M−20%-FILLER could be mainly due to the lower quantity of cement in the mix, as well as to the fact that it has been lost a somewhat toughening effect of the sand and due to the high porosity of samples caused by the difficulty in casting and compaction given by an almost null workability of the mixture.

Compressive strength test

Fig. 12-a shows the compressive strength obtained in the case in which PE resin has been employed as partial replacement of PLC, highlighting the same strength reduction already highlighted with reference to flexural strength. 5% replacement by volume does not significantly affect the compressive strength, resulting into a percentage reduction always lower than 5% (the low amount of PE particles does not alter the micro-structure of mortar). Increasing the level of substitution up to 10% and 20%, the compressive strength starts to decrease with a hypothesized trend proportional to 75% of the level of substitution. At 3 days, it has been found the maximum decrease in strength equal to −18.11% and −20.50% respectively for M−10%-PL and M−20%-PL. After this curing age, the percentage variation is lower, and it stabilizes at around −15% for M−20%-PL and −7% for M−10%-PL (except for 28 days where it is −14.01%). Also in this case, the results seem to confirm the presence of a seed effect and this, at least for the 5%-

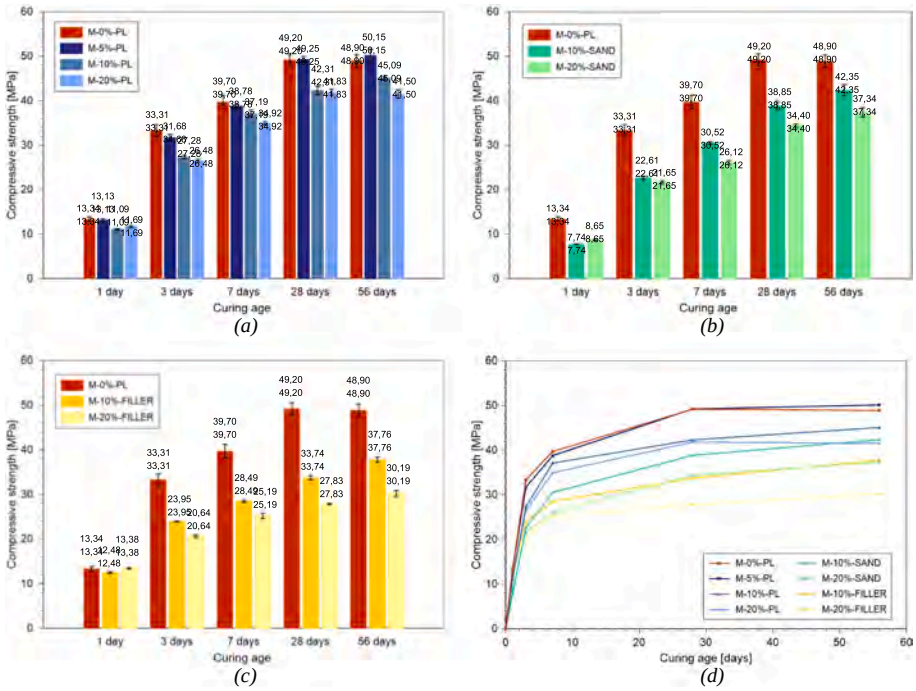

Fig. 12. Compressive strength for mortars having PLC substitution (a), sand substitution (b) or PE used as filler (c) at different levels of substitution and global superimposing of results (d).

PL mix, does not lead to any significant variation. At higher levels of substitution this effect vanishes, especially in the longer term.

In the case of PE in partial substitution of sand, Fig. 12-b shows that, at all the curing ages, the compressive strength of reference mix is the highest and the difference with the mixtures containing PE resin particles is very large. At 28 days the percentage reduction is equal to −21.03% for M−10%-SAND and −30.07% for M−20%-SAND. The reasons of the high reduction are likely the lower stiffness of PE particles as compared to that of sand grains and the smoother surface of the former as compared to the latter, together with their smallest size, resulting into a lower interlocking effect between constituents and hence a lower and less effective crack-arrestor action. As in the case of flexural strength, the percentage reduction of compressive strength is a bit recovered with aging, confirming a possible delaying in the hydration of cement when PE resin particles partially substitute sand, which, however, needs to find further confirmation.

Compressive strength results obtained in the case in which PE resin has been employed as filler are shown in Fig. 12-c. At 24 h, compressive strength shows no significant variation among the mixes. The maximum variation concerns M−10%-FILLER with a percentage reduction equal to −6.42%. Starting from 3 days of curing, the differences with the reference mix start increasing. At 28 days, the reference mix showed a compressive strength of 49.20 MPa while M−10%-FILLER and M−20%-FILLER mixes obtained a value of 33.74 MPa and 27.83 MPa which bring to a percentage reduction equal to −21.03% and −30.07% respectively.

Shrinkage deformation and mass variation

The time evolution of shrinkage deformation for all the investigated mortar specimens is reported in Fig. 13-a.

When PE resin particles are employed in partial substitution of PLC, the mixtures are subjected to a lower shrinkage compared to the reference. Considering the percentage variation at stabilization (83 days), it

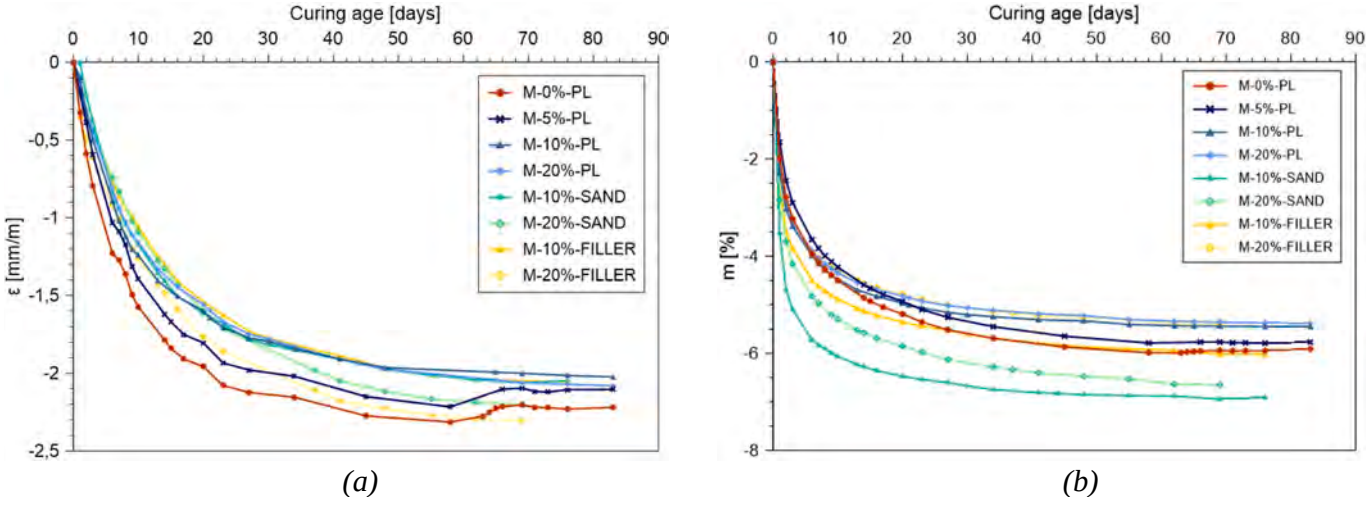

Fig. 13. Shrinkage deformation (a) and mass variation (b) for mortars having PE resin at different levels of substitution and in substitution to different constituents.

is equal to −5.4% in M−5%-PL, −8.5% in M−10%-PL and −6.3% in M−20%-PL. Generally, it can be said that using PE resin particles in partial substitution of PLC results into a negligible reduction in shrinkage deformation and it is mainly due to the lower amount of water in the mixtures whose evaporation is the cause of shrinkage.

When PE resin particles substitute part of sand, the mixtures exhibit a slightly lower shrinkage with respect to the reference mix. However, M−20%-SAND stabilizes at a percentage reduction equal to −0.9% (at 69 days) that is less than the one of M−10%-SAND equal to −7.5% (at 76 days). As in the case of replacement by volume of PLC, the addition of PE resin reduces the shrinkage in a negligible way.

When PE resin is used as filler of a total volume percentage, the shrinkage strain shows opposite behavior for the two chosen percentages. With respect to M−0%-PL, M−10%-FILLER has a lower deformation with a reduction equal to −7.6% (at 76 days). while M−20%-FILLER has a higher deformation with an increment of + 5.5% (at 69 days). This is likely caused by a sort of random defectiveness in the casting and compaction of the mixture. However, considering both percentage variation and deformation, the effect of PE resin is negligible.

Reported in Fig. 13-b, the mass variation of the whole specimens has been monitored during their drying. For PLC partial substitution, mass variation is coherent with the shrinkage evaluation. The higher the substitution, the lower the mass variation. The mass variation stabilized at −5.91% for M−0%-PL, −5.77% for M−5%-PL, −5.45% for M−10%-PL and −5.38% for M−20%-PL.

Partial sand replacement with PE resin results into an opposite behavior of mass variation with respect to the shrinkage evaluation. The reference specimen has the lowest variation, while M−10%-SAND and M−20%-SAND stabilized at −6.91% and −6.65% respectively.

When PE resin is used as filler, opposite to the shrinkage deformation, comparing to the reference mix it is M−20%-FILLER the one with lower mass variation (-5.39%) and M−10%-FILLER the one with higher value (-6.03%). As in the case of sand replacement, these inconsistent results could be explained by too high quantity of PE resin which completely modifies the interaction in the micro-structure between the constituents compared to the reference case or by defects during casting specimens.

In any case, the small difference between results show that the addition of PE resin does not affect significantly mass variation.

Calorimetric test

Since compressive and flexural strength values at early stage are very similar among all the specimens, it has been hypothesized that PE resin particles provide a seed effect in the hydration process of PLC promoting such reaction. Thus, calorimetric tests have been performed to verify this statement. Looking at the evolution of the hydration temperature produced during the adiabatic reaction (Fig. 14), it can be seen an increment in hydration temperature as the amount of PE resin added in the mixture increases. The temperature reached by M−0%-PL is 84.6 °C, while for M−10%-PL and M−10%-SAND it is 87.3 °C and 90.8 °C. This increment in temperature indicates a higher hydration that might further confirms the statement for which PE resin particles act as seed of the hydration process but then their effect vanishes with aging.

Fluorescence analysis

Through fluorescent microscope analysis (Fig. 15), it has been observed a quite homogenous distribution of PE resin particles both in the fractured and cut side of mortar samples, making sure that no preferential sections of rupture are created. A further confirmation has been obtained through stereomicroscope analysis (Fig. 16) where, other than the spatial distribution of PE resin (colored in blue/gray), it is visible the different and higher PE resin quantity that is embedded in the cement matrix of the four mortar mixes analyzed in this research. The higher the amount of PE resin, the darker the cement matrix.

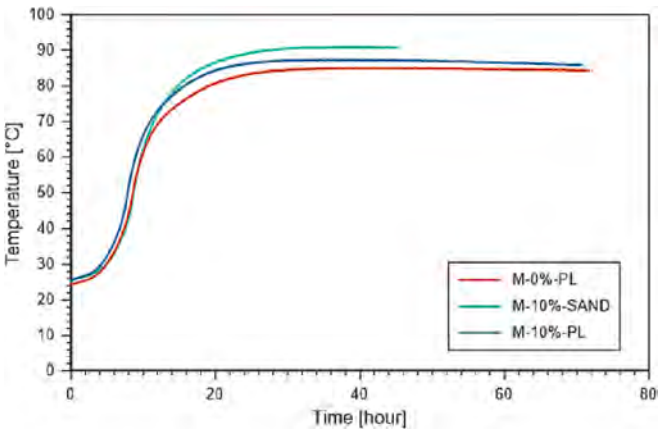

Fig. 14. Calorimetric test output for mortars having 10% by volume substituted by PLC or sand.

Thermo-gravimetric (TGA) analysis

In TGA analysis, similar trends have been obtained for all the specimens (Fig. 17). After a first weight variation at 100 °C attributable to the loss of water in the specimen, other weight losses are detectable at 400 °C where portlandite ($Ca(OH)_2$) is decomposed and at 800 °C which corresponds with the decompositions of the calcium carbonate ($CaCO_3$). For a 10% substitution, the trend is very similar to the reference, while when the level of substitution increases to 20% the loss in weight is higher. Moreover, the higher the amount of PE resin present in the sample, the higher is the percentage of weight loss. It is known that thermal decomposition of PE starts at temperature higher than 219 °C. The results of TGA analysis are very interesting but not clear at all, they are likely to confirm the seed hydration effect. In fact, since $Ca(OH)_2$ and $CaCO_3$ are cement hydration by-products, the analysis outcome that these elements degrade more in TGA could demonstrates that PE resin in partial substitution of natural constituents promotes the cement hydration. Instead, when PE resin partially substitutes PLC, no variations are recognizable because the seed effect is compensated by the global decreasing of PLC.

Scanning electronic microscope (SEM) analysis

Analyzing SEM images of mortar samples (Fig. 18) it has been firstly observed small voids at both cement paste-aggregate and cement paste-PE resin interfaces. The substantial difference that has been found between the two interfaces is that in the first case, the rough surface of sand creates an indented profile at interface with cement matrix, which reflects in a good and compact bonding with no voids between elements. Instead, the smooth surface of PE resin makes the interface almost straight, bringing to a lack of interlocking effect and favoring an early detachment of component which is also visible from EDS spectrum where, differently from sand (colored in blue), PE resin (colored in pink) has no calcium (colored in grey and identifying cement matrix) on its surface. All these results, corroborate what has been found by mechanical test where the mechanical strength reduction is mainly caused by the weaker cement matrix-PE resin interface.

Scale-up to concrete

Among all the mortar mixes previously analyzed in Section 3.2, the one having the most consistent values with each other and recording the lowest decrease in mechanical properties are those with Portland Limestone Cement (PLC) substitution. The chosen one to be replicated in concrete is the one with PE resin as 20% replacement by volume, since it has been considered acceptable the reduction of mortar compressive strength at 28 days equal to −15% and adequate the level of volume replacement of 20% that in the case of the investigated concrete mixture

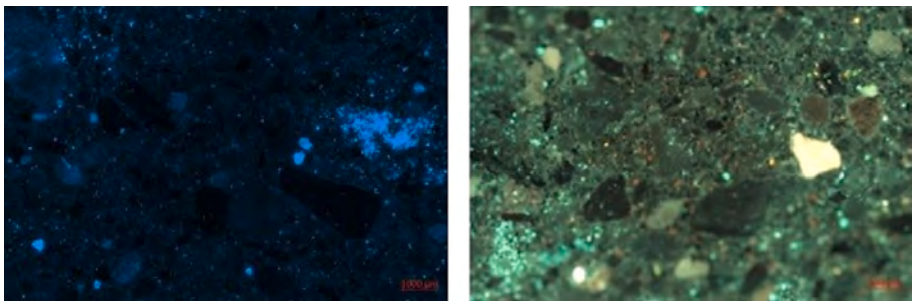

Fig. 15. Fluorescence test output (JRC Ispra). Fractured side on the left, cut side on the right.

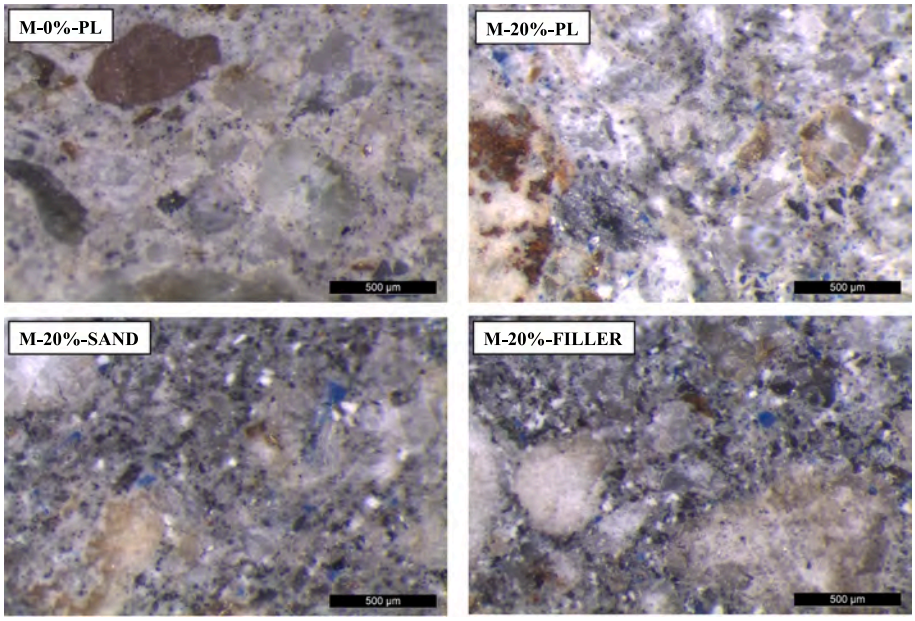

Fig. 16. Stereomicroscope images of mortars (x50).

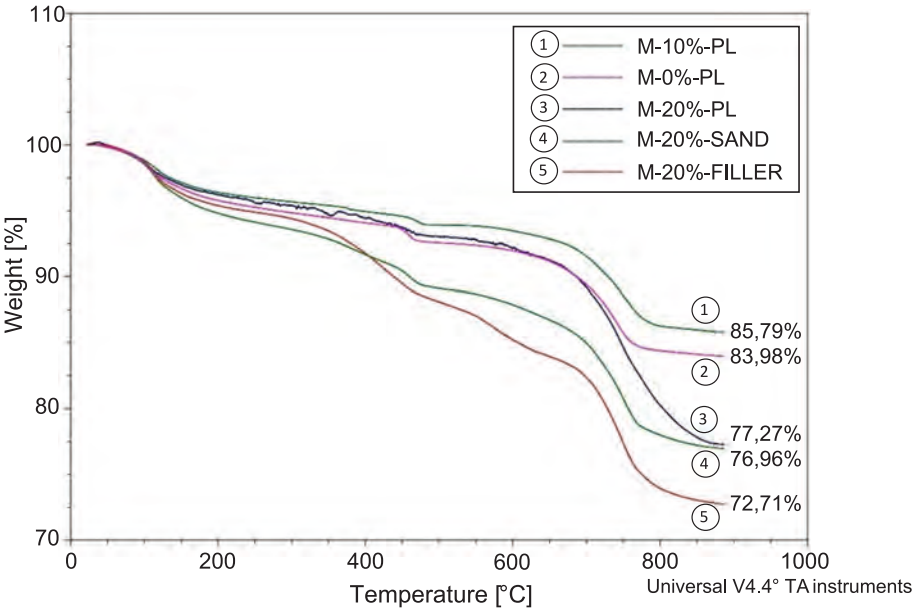

Fig. 17. TGA analysis output (JRC Ispra).

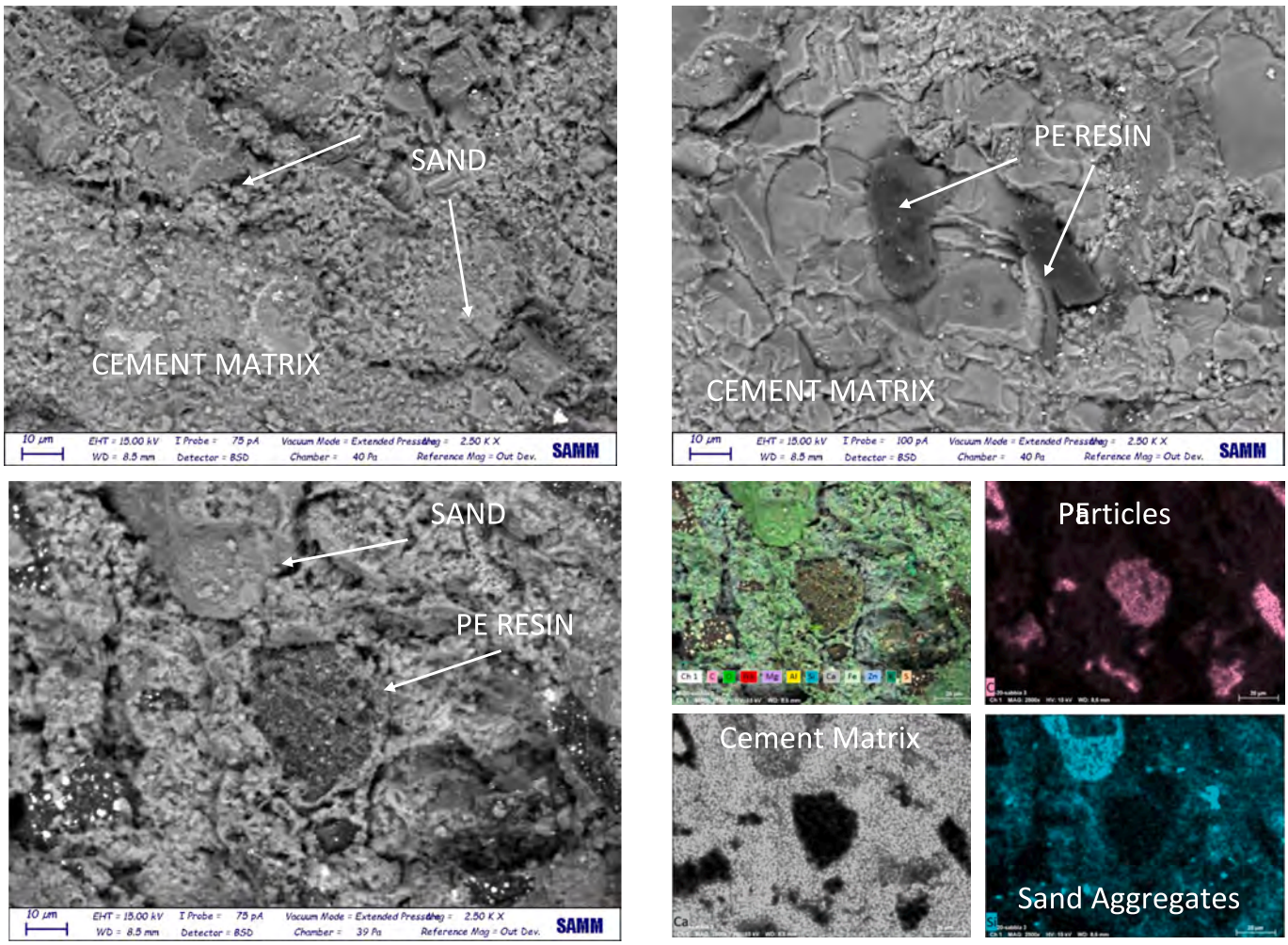

Fig. 18. SEM images and EDS spectrum of cement paste- PE resin and aggregate interfaces.

brings to utilize 36.9 kg/m^3 of PE resin saving 28 kg/m^3 of PLC. With respect the total volume of cement and PE resin, the PE resin is present at 10% by mass. Furthermore, besides reporting the experimental results, a comparison has been also carried out with the corresponding values proposed by Eurocode 2 (EC2) to evaluate the agreement of the tested concrete to Code prescription.

Rheometer tests

Flow curve test results, reported in Fig. 19-a, provide an indication of the influence of the cement replacement by PE resin particles on the Bingham parameters of dynamic yield stress τ_0 and plastic viscosity μ, which are respectively related to the torque value and to the viscosity value (curve slope). τ_0 is higher in the reference mix (211.94 Pa compared to 163.25 Pa of C-20%-PL), while μ is higher in the C-20%-PL mixture (33.02 Pa • s compared to 12.48 Pa • s of the reference). The static yield stress is instead evaluated trough the stress growth test (Fig. 19-b). Its value is lower in the reference mix (233.79 Pa and 294.69 Pa respectively) confirming the findings already highlighted from slump-flow diameter and efflux test results on cement pastes and mortars.

This is mainly due to the hydrophilicity of the PE resin particles, but also due to the establishment of a filler effect caused by PE resin powder that thickens the cement paste when it is added into concrete.

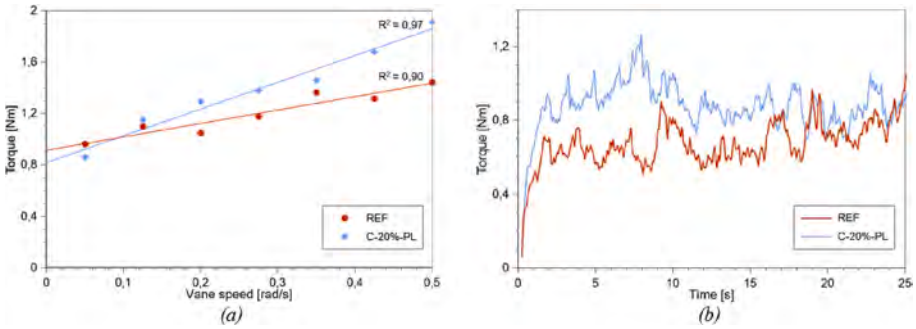

Fig. 19. Concrete flow curve test (a) and stress growth test (b).

Compressive strength

Fig. 20 reports the values of cubical (R_c) and cylindrical (f_c) compressive strength of the specimens. As expected, the presence of PE resin particles in the mix leads to an almost constant reduction in compressive strength of about 20% at all the curing ages. Evaluated at 28 days, the percentage reduction is equal to −19.49% in R_c case, which lowered to −18.59% in the case of f_c.

Referring to EC2, two different checks have been made for the validation of the experimental results. It has been first computed the *fc/Rc* ratio which was then compared to the value 0.83 given by the standard finding a maximum absolute error equal to 4.4%, experimentally negligible. Secondly, in accordance with EC2 part 3.1.2 the mean compressive strength $f_{cm}(t)$ has been estimated at various ages *t*, starting from the mean strength at 28 days f_{cm}, as indicated by equation (11):

$$f_{cm}(t) = \beta_{cc}(t) \bullet f_{cm} \quad with \quad \beta_{cc}(t) = exp(s(1 - (28/t)^{\frac{1}{2}})) \tag{11}$$

Considering f_{cm} as the experimental cylindrical compressive values at 28 days and the coefficient *s* equal to 0.2, the estimated cylindrical compressive strengths have been reported in Fig. 20-b together with the experimental ones. Compared to EC2, the maximum positive variation has been found in REF specimens (+5.51% at 7 days), while the maximum negative variation has been found for C-20%-PL specimens (-4.65% at 56 days). Therefore, it can be concluded that the tests were correctly carried out and that PE resin addition does not move the values away from the EC2 prediction even if it is calibrated on ordinary concrete. Further supported by the results obtained for mortar, it can be also hypothesized that the percentage reduction of compressive strength, which could be explained both by a lower PLC content and by a weaker interface between cement paste and PE resin (as shown in Subsection 3.2.9 above), is directly proportional to the percentage of PE resin particles integrated in the mix.

Flexural strength and fracture energy

PE resin particles in partial replacement of PLC results into a reduction in concrete flexural strength at each curing age too (Fig. 21-a). At 28 days the flexural strength has been evaluated equal to 4.15 MPa (REF) and 3.25 MPa (C-20%-PL) with a percentage reduction in strength of −20.95%, which could be mainly caused by the internal appearance of the specimens visible after the failure: differently from REF, the rupture section of C-20%-PL specimens has several well distributed micro-pores that weaken its internal structure (Fig. 21-b), whose presence can be justified considering that the film of water which surrounds the PE particles evaporates after aging.

An additional parameter that has been calculated from flexural test results is the fracture energy that is the energy required by the specimen to break. Reported in Fig. 22, fracture energy has been calculated as the area subtended by the load-CMOD curve (directly created during the test acquiring CMOD with the clip gauge, for example Fig. 23 shows the load-CMOD curve at 7 days) up to a fixed crack mouth opening displacement equal to 1,5 mm. Comparing the results of C-20%-PL specimens with respect to REF ones, the measured fracture energy is lower. As expected, plastic particles do not give benefits in toughness since their powdery granulometry and "glassy" particle texture. Though at 28 days of curing a fracture energy of C-20%-PL samples comparable to the one of REF (+2.05%) has been obtained, the higher standard deviation may suggest, as observed, a non-homogeneous distribution of micro-pores in the specimens.

Elastic modulus

In Fig. 24, the elastic modulus results show the degradation of the stiffness as the PE resin is incorporated in the mixture resulting into a percentage reduction at 28 days equal to −16.79%. Moreover, in case of C-20%-PL no significant increase of stiffness occurred during the whole curing period. Once again, the reason could be identified in the lower interface quality between constituents.

For the validation of these results, a comparison has been done with respect to the values estimated in Eurocode 2 part 3.1.3. Starting from mean compressive strength f_{cm} [MPa] at 28 days, the elastic modulus $E_m(t)$ at any age *t* is expressed in MPa as indicated by equation (12):

$$E_{c,s}(t) = \left(\frac{f_{cm}(t)}{f_{cm}}\right)^{0.3} \bullet E_{cm} \quad with \quad E_{cm} = 22000(f_{cm}/10)^{0.3} \tag{12}$$

Considering *fcm(t)* as the experimental cylindrical compressive values, the predicted values are reported and compared to the experimental ones in Fig. 24. C-20%-PL samples report a slightly higher difference with respect to EC2 (-10.14% at 28 days), however justifiable by the composition of the concrete, alien to the database on which empirical EC2 relationship has been calibrated.

Shrinkage deformation

Shrinkage deformation has been monitored up to the full stabilization of the deformation, which occurred 78 days after casting (Fig. 25). C-20%-PL mixture initially had a lower shrinkage compared to the reference mix, but when the deformation starts to stabilize, after about 45 days, there is a trend reversal of the deformations. At 28 days, C-20%-PL has a shrinkage deformation 8.36% lower than REF (higher variation among all the period), while at stabilization the variation has been evaluated equal to + 3.26%. In any case, considering the difference between them, the variation in shrinkage deformation is negligible (±0.01 mm/m).

Even in the case of shrinkage strain, the experimental values have been compared to the one estimated by Eurocode 2 part 3.1.4. EC2 estimates the total shrinkage strain as the sum of two components: the drying shrinkage strain ε_{cd}, function of the migration of the water through the hardened concrete, plus the autogenous shrinkage strain ε_{ca}, linear function of the characteristic concrete strength f_{ck}. Hence, the values of shrinkage strain ε_{cs} at any time *t* has been evaluated as $\varepsilon cs(t) = \varepsilon cd(t) + \varepsilon ca(t)$, singularly expressed as indicated by equations (13) and (14):

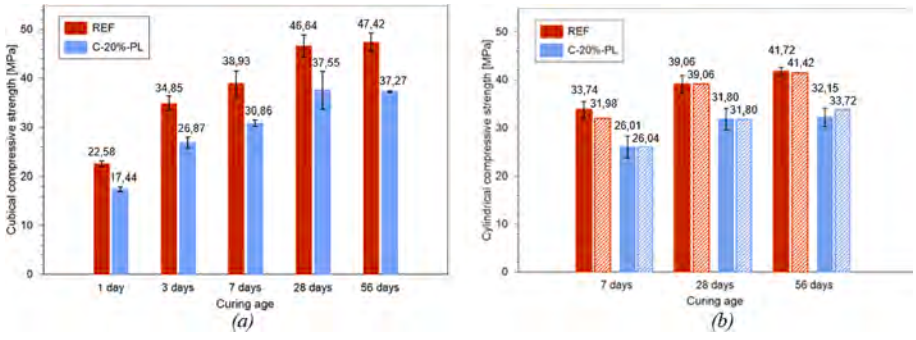

Fig. 20. Concrete cubical compressive strength (a). Concrete cylindrical compressive strength (b). Solid = Experimental value, Dashed = EC2 prediction.

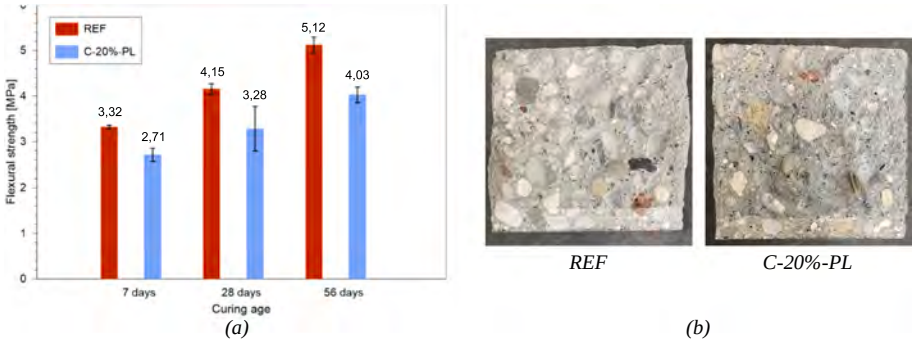

Fig. 21. Concrete flexural strength values.

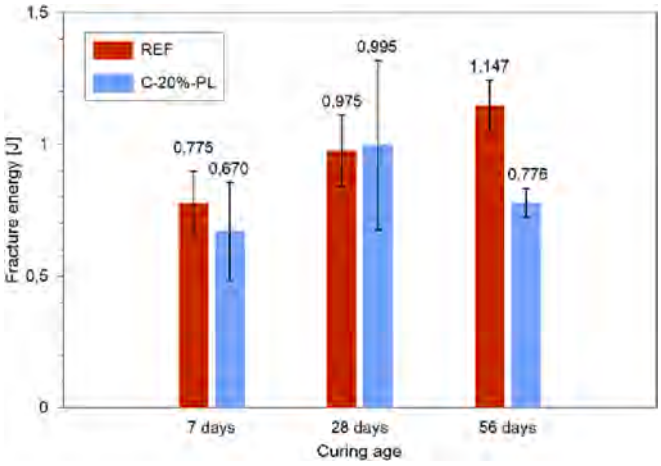

Fig. 22. Concrete fracture energy.

$$\varepsilon_{cd}(t) = \beta_{ds}(t,t_s) \bullet k_h \bullet \varepsilon_{cd,0} \quad with \quad \beta_{ds}(t,t_s) = \frac{t-t_s}{(t-t_s)+0.04\sqrt{h_0^3}} \tag{13}$$

$$\varepsilon_{ca}(t) = \beta_{as}(t) \bullet \varepsilon_{ca,inf} \quad with \quad \beta_{as}(t) = 1 - exp\left(-0.2t^{0.5}\right); \quad \varepsilon_{ca,inf} = 2.5(f_{ck}-10)10^{-6} \tag{14}$$

In Fig. 25 is clearly visible how the experimental values are close to the estimation (lower 10%), demonstrating both the accuracy of the casting and testing procedures and, especially, the validity of the EC2 prediction formulas.

Conclusions

The detailed study reported in this paper leads to a number of conclusions, which in general allow to state that, even if gamma irradiation process is not effective for Polyester (PE) resin, using PE resin plastic particles in cement-based materials as partial substitution of their natural constituents (in particular Ordinary Portland Cement) could be a valid application to reduce carbon footprint of these materials and decrease the amount of non-recycled plastic waste, while maintaining an acceptable level of performance of the obtained cementitious composite.

Based on the experimental findings of the first part of the work, all the mechanical and physical properties (apart from viscosity of cement pastes) do not register a significant variation between the cement pastes

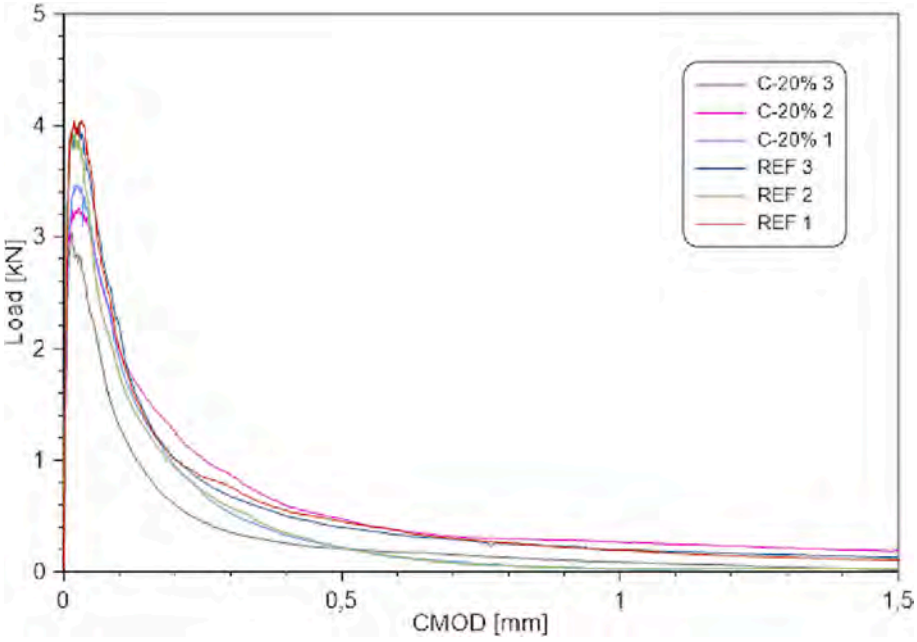

Fig. 23. Load-CMOD curve at 7 days of curing.

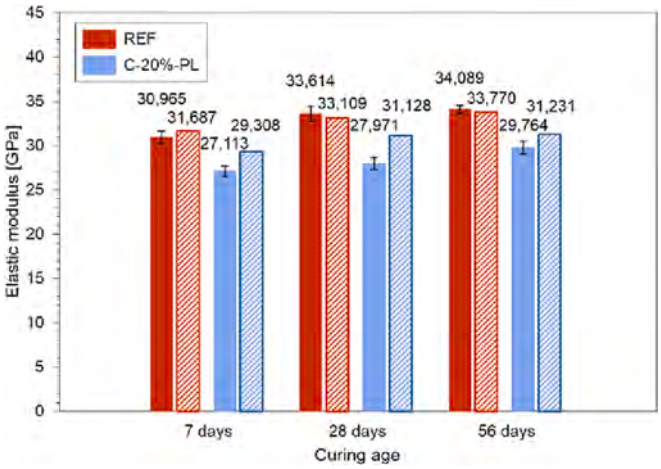

Fig. 24. Concrete elastic modulus. Solid = Experimental value, Dashed = EC2 prediction.

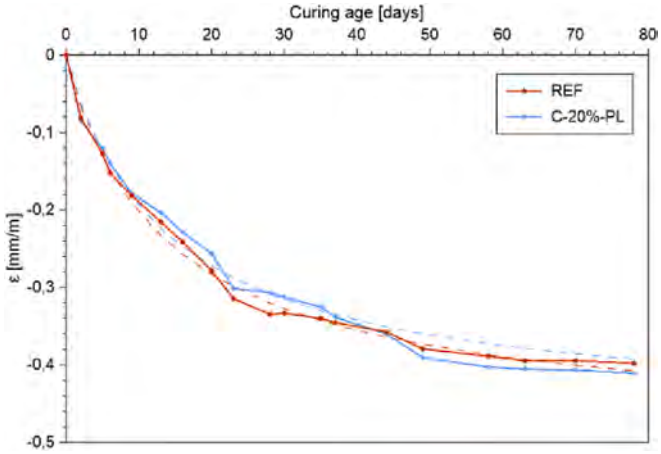

Fig. 25. Concrete shrinkage deformation. Solid = Experimental value, Dashed = EC2 prediction.

or mortars containing non-irradiated particles and the ones containing 10 KGy or 100 KGy irradiated particles. Therefore, it can be concluded that the use of PE resin subjected to gamma irradiation process instead of non-irradiated particles is not relevant to the recovery or improvement of mechanical properties when they are used in partial substitution of Ordinary Portland Cement. This might be because of the PE resin particles size that is too small ($\approx$3.5 μm) to increase their microstructural crystallinity when subjected to the gamma irradiation process or, differently from PET, this type of process is ineffective on PE resin. Furthermore, it has been found that the use of plastic particles as 5% by volume replacement of Ordinary Portland Cement does not significantly reduce the mechanical and physical properties of cement pastes and mortar. This may be due to the particle finesses (higher than that of PLC) and the amount of added PE resin that are too small to interfere with the other constituents so as not to weaken the material micro-structure. Thus, it is reasonable to increase the level of substitution, increasing both the saving of raw material and the recycling of plastic waste.

The outcomes of the second part, asserted that the addition of PE resin particles at higher volume replacement ratio and at any substitution combination, results into a loss of mortar mechanical and physical performance, which worsen when the level of substitution increases. PE resin used as filler is the worst solution that always feature the highest reduction in strength and workability, then followed by sand substitution (which is however the one with lowest loss of workability) and PLC substitution, which is considered the most suitable solution. In terms of workability, more than the sole PE resin additive, it is the lower amount of water in the mixture that mainly reduces such property, while the reduction of mechanical properties has been supposed mainly due to the lower PLC content as well as to the weaker PE resin-cement paste interface, lower stiffness, lower interlocking effect of PE resin compared to natural raw constituents.

From these results, a dependency between loss of strength and difference in grain dimension between PE resin particles and the corresponding substituted natural constituent has been identified. The lower the difference in grain dimension, the lower the loss of strength. Moreover, when PE resin is used in partial substitution of PLC, the likely presence of a "seed effect" has been identified. This effect accelerates the cement hydration producing an early-stage strength of the material comparable to the reference one. More visible for 5% substitution by volume, the effect vanishes when the level of substitution increases and the age increases, since its benefit is balanced by the lower content of cement in the mixtures.

The final step of the research was meant to ascertain if PE resin can be effectively used as a component in a mix design suitable for structural applications. In order to comply with acceptable levels of both reduction of mechanical properties and substitution of cement, a concrete mix where 20% by volume of PLC was substituted with PE resin particles was studied, starting from a reference mix. The addition of PE resin particles into the concrete mix resulted into a concrete more viscous and with a higher yield stress, with almost equal shrinkage deformation and a reduction of compressive strength (-19.49% and −18.59% respectively for R_c and f_c at 28 days) and flexural strength (-20.96% at 28 days) substantially proportional to the level of cement replacement substitution (20%) and constant at each curing ages. Consistent with the variation of the compressive strength, even the elastic modulus undergoes a reduction equal to −16.79% at 28 days.

In conclusion, even if the 20% by volume substitution of PLC with recycled PE resin particles does not brings benefits in mechanical performance and material toughness (PE resin has a too powdery granulometry), the research provides interesting results about the possibility of reusing economically viable quantities of PE resin into concrete while still being able to produce concrete with hardened state performance sound for structural applications. Further verification of the technical feasibility of this approach will require durability studies of the investigated concrete mixes as well as the use of supplementary cementitious materials also as a partial compensation of the negative effects due to the incorporation of PE resin particles.

Declaration of Competing Interest

The authors declare that they have no known competing financial interests or personal relationships that could have appeared to influence the work reported in this paper.

Data availability

Data will be made available on request.

Acknowledgements

The work has been conducted in the framework of the project Sustainable Efficient Alternative Plastic Storage (SEAPLAST) funded by the Joint Research Centre under the Exploratory Research scheme. The help of Mr. Massimo Iscandri (Laboratory for Testing Materials, Buildings and Structures, Politecnico di Milano) in casting specimens for the experimental programme and providing organizational support for its execution is gratefully acknowledged.

References

Akçaözoğlu, S., Atiş, C.D., Akçaözoğlu, K., 2010. An investigation on the use of shredded waste PET bottles as aggregate in lightweight concrete. Waste Manag. 30 (2), 285–290. https://doi.org/10.1016/j.wasman.2009.09.033.

Akçaözoğlu, S., Akçaözoğlu, K., Atiş, C.D., 2013. Thermal conductivity, compressive strength and ultrasonic wave velocity of cementitious composite containing waste PET lightweight aggregate (WPLA). Compos. Part B Eng. 45 (1), 721–726. https://doi.org/10.1016/j.compositesb.2012.09.012.

Albano, C., Camacho, N., Hernández, M., Matheus, A., Gutiérrez, A., 2009. Influence of content and particle size of waste pet bottles on concrete behavior at different w/c ratios. Waste Manag. 29 (10), 2707–2716. https://doi.org/10.1016/j.wasman.2009.05.007.

Almeshal, I., Tayeh, B.A., Alyousef, R., Alabduljabbar, H., Mustafa Mohamed, A., Alaskar, A., 2020. Use of recycled plastic as fine aggregate in cementitious composites: A review. Constr. Build. Mater. 253, 119146 https://doi.org/10.1016/j.conbuildmat.2020.119146.

Azhdarpour, A.M., Nikoudel, M.R., Taheri, M., 2016. The effect of using polyethylene terephthalate particles on physical and strength-related properties of concrete; A laboratory evaluation. Constr. Build. Mater. 109, 55–62. https://doi.org/10.1016/j.conbuildmat.2016.01.056.

Basha, S.I., Ali, M.R., Al-Dulaijan, S.U., Maslehuddin, M., 2020. Mechanical and thermal properties of lightweight recycled plastic aggregate concrete. J. Build. Eng. 32, 101710.

Belmokaddem, M., Mahi, A., Senhadji, Y., Pekmezci, B.Y., 2020. Mechanical and physical properties and morphology of concrete containing plastic waste as aggregate. Constr. Build. Mater. 257, 119559.

L. Bertolini and M. Carsana, *Materiali da Costruzione*, 3rd ed. De Agostini Scuola, 2014.

Borg, R.P., Baldacchino, O., Ferrara, L., 2016. Early age performance and mechanical characteristics of recycled PET fibre reinforced concrete. Constr. Build. Mater. 108, 29–47. https://doi.org/10.1016/j.conbuildmat.2016.01.029.

Brooks, A.L., Wang, S., Jambeck, J.R., 2018. The Chinese import ban and its impact on global plastic waste trade. Sci. Adv. 4 (6), 1–8. https://doi.org/10.1126/sciadv.aat0131.

Degnan, T., Shinde, S.L., 2019. Waste-plastic processing provides global challenges and opportunities. MRS Bull. 44 (06), 436–437.

del Rey Castillo, E., Almesfer, N., Saggi, O., Ingham, J.M., 2020. Light-weight concrete with artificial aggregate manufactured from plastic waste. Constr. Build. Mater. 265, 120199.

Plastics Europe, "Plastics – the Facts 2020. An analysis of European plastics production, demand and waste dara," 2020. [Online]. Available: https://www.plasticseurope.org/application/files/3416/2270/7211/Plastics_the_facts-WEB-2020_versionJun21_final.pdf%0Ahttps://www.plasticseurope.org/en/resources/publications/4312-plastics-facts-2020.

Faraj, R.H., Sherwani, A.F.H., Daraei, A., 2019. Mechanical, fracture and durability properties of self-compacting high strength concrete containing recycled polypropylene plastic particles. J. Build. Eng. 25, 100808.

Federbeton, "Rapporto di Filiera 2020," 2020.

Federbeton, "Rapporto di Sostenibilità 2020," 2020.

Ferreira, L., De Brito, J., Saikia, N., 2012. Influence of curing conditions on the mechanical performance of concrete containing recycled plastic aggregate. Constr. Build. Mater. 36, 196–204. https://doi.org/10.1016/j.conbuildmat.2012.02.098.

Foti, D., 2011. Preliminary analysis of concrete reinforced with waste bottles PET fibers. Constr. Build. Mater. 25 (4), 1906–1915. https://doi.org/10.1016/j.conbuildmat.2010.11.066.

Foti, D., 2013. Use of recycled waste pet bottles fibers for the reinforcement of concrete. Compos. Struct. 96, 396–404. https://doi.org/10.1016/j.compstruct.2012.09.019.

Frigione, M., 2010. Recycling of PET bottles as fine aggregate in concrete. Waste Manag. 30 (6), 1101–1106. https://doi.org/10.1016/j.wasman.2010.01.030.

Geyer, R., Jambeck, J.R., Law, K.L., 2017. Production, use, and fate of all plastics ever made. Sci. Adv. 3 (7), 25–29. https://doi.org/10.1126/sciadv.1700782.

Gu, L., Ozbakkaloglu, T., 2016. Use of recycled plastics in concrete: A critical review. Waste Manag. 51, 19–42. https://doi.org/10.1016/j.wasman.2016.03.005.

Hannawi, K., Kamali-Bernard, S., Prince, W., 2010. Physical and mechanical properties of mortars containing PET and PC waste aggregates. Waste Manag. 30 (11), 2312–2320. https://doi.org/10.1016/j.wasman.2010.03.028.

Kim, J.H.J., Park, C.G., Lee, S.W., Lee, S.W., Won, J.P., 2008. Effects of the geometry of recycled PET fiber reinforcement on shrinkage cracking of cement-based composites. Compos. Part B Eng. 39 (3), 442–450. https://doi.org/10.1016/j.compositesb.2007.05.001.

Kim, S.B., Yi, N.H., Kim, H.Y., Kim, J.H.J., Song, Y.C., 2010. Material and structural performance evaluation of recycled PET fiber reinforced concrete. Cem. Concr. Compos. 32 (3), 232–240. https://doi.org/10.1016/j.cemconcomp.2009.11.002.

J. Lehne and F. Preston, "Making Concrete Change: Innovation in Low-carbon Cement and Concrete," *Chatham House*, 2018.

Marzouk, O.Y., Dheilly, R.M., Queneudec, M., 2007. Valorization of post-consumer waste plastic in cementitious concrete composites. Waste Manag. 27 (2), 310–318. https://doi.org/10.1016/j.wasman.2006.03.012.

Ochi, T., Okubo, S., Fukui, K., 2007. Development of recycled PET fiber and its application as concrete-reinforcing fiber. Cem. Concr. Compos. 29 (6), 448–455. https://doi.org/10.1016/j.cemconcomp.2007.02.002.

Pereira De Oliveira, L.A., Castro-Gomes, J.P., 2011. Physical and mechanical behaviour of recycled PET fibre reinforced mortar. Constr. Build. Mater. 25 (4), 1712–1717. https://doi.org/10.1016/j.conbuildmat.2010.11.044.

Rahmani, E., Dehestani, M., Beygi, M.H.A., Allahyari, H., Nikbin, I.M., 2013. On the mechanical properties of concrete containing waste PET particles. Constr. Build. Mater. 47, 1302–1308. https://doi.org/10.1016/j.conbuildmat.2013.06.041.

H. Ritchie and M. Roser, "Plastic Pollution," *Our world Data*, 2018.

Sadrmomtazi, A., Dolati-Milehsara, S., Lotfi-Omran, O., Sadeghi-Nik, A., 2016. The combined effects of waste Polyethylene Terephthalate (PET) particles and pozzolanic materials on the properties of selfcompacting concrete. J. Clean. Prod. 112, 2363–2373. https://doi.org/10.1016/j.jclepro.2015.09.107.

Saikia, N., De Brito, J., 2014. Mechanical properties and abrasion behaviour of concrete containing shredded PET bottle waste as a partial substitution of natural aggregate. Constr. Build. Mater. 52, 236–244. https://doi.org/10.1016/j.conbuildmat.2013.11.049.

Schaefer, C.E., Kupwade-Patil, K., Ortega, M., Soriano, C., Büyüköztürk, O., White, A.E., Short, M.P., 2018. Irradiated recycled plastic as a concrete additive for improved chemo-mechanical properties and lower carbon footprint. Waste Manag. 71, 426–439.

Silva, D.A., Betioli, A.M., Gleize, P.J.P., Roman, H.R., Gómez, L.A., Ribeiro, J.L.D., 2005. Degradation of recycled PET fibers in Portland cement-based materials. Cem. Concr. Res. 35 (9), 1741–1746. https://doi.org/10.1016/j.cemconres.2004.10.040.

Silva, R.V., De Brito, J., Saikia, N., 2013. Influence of curing conditions on the durability-related performance of concrete made with selected plastic waste aggregates. Cem. Concr. Compos. 35 (1), 23–31. https://doi.org/10.1016/j.cemconcomp.2012.08.017.

Thorneycroft, J., Orr, J., Savoikar, P., Ball, R.J., 2018. Performance of structural concrete with recycled plastic waste as a partial replacement for sand. Constr. Build. Mater. 161, 63–69. https://doi.org/10.1016/j.conbuildmat.2017.11.127.

Umasabor, R.I., Daniel, S.C., 2020. The effect of using polyethylene terephthalate as an additive on the flexural and compressive strength of concrete. Heliyon 6 (8), e04700.

United Nations, 2018. The state of plastics: World Environment Day Outlook 2018. UN Environ. Program. https://doi.org/10.1093/oxfordhb/9780199238804.003.0031.

United Nations, 2021. "2021 Global Status Report for Buildings and Construction", *UN Environ.* Program.